

การศึกษาเชิงทฤษฎีของการปิดวงแหวนภายในโมเลกุลของแอมิโนคีโตนและแอลดีไฮด์เป็นอนุพันธ์ควิโนลิโนน
เร่งปฏิกิริยาด้วยแอล-โพรลีน



นาย ปริญญา หงษ์ทอง

สถาบันวิทยบริการ จุฬาลงกรณ์มหาวิทยาลัย

วิทยานิพนธ์นี้เป็นส่วนหนึ่งของการศึกษาตามหลักสูตรปริญญาวิทยาศาสตรมหาบัณฑิต

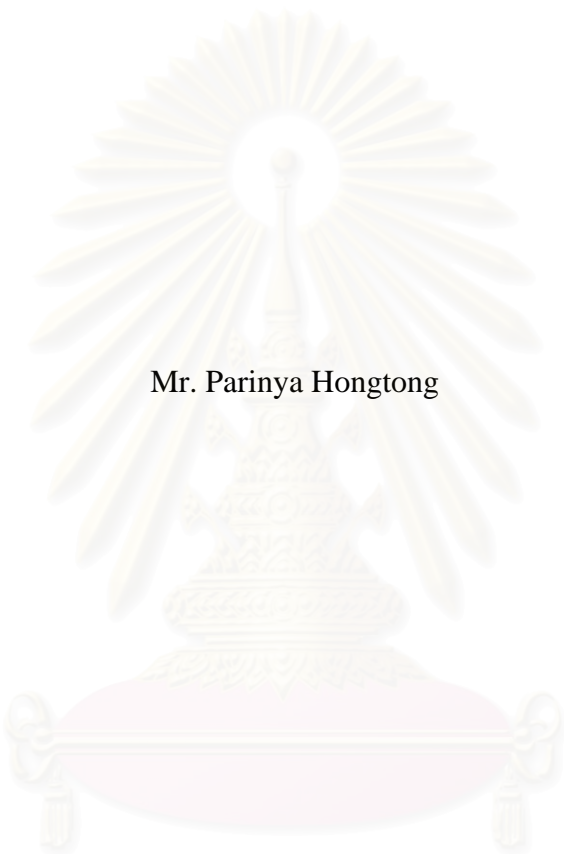
สาขาวิชาปิโตรเคมีและวิทยาศาสตร์พอลิเมอร์

คณะวิทยาศาสตร์ จุฬาลงกรณ์มหาวิทยาลัย

ปีการศึกษา 2550

ลิขสิทธิ์ของจุฬาลงกรณ์มหาวิทยาลัย

THEORETICAL STUDY ON L-PROLINE-CATALYZED INTRAMOLECULAR
CYCLIZATION OF AMINOKETONE AND ALDEHYDE TO
QUINOLINONE DERIVATIVES



Mr. Parinya Hongtong

สถาบันวิทยบริการ

จุฬาลงกรณ์มหาวิทยาลัย

A Thesis Submitted in Partial Fulfillment of the Requirements
for the Degree of Master of Science Program in Petrochemistry and Polymer Science

Faculty of Science


Chulalongkorn University

Academic Year 2007

Copyright of Chulalongkorn University


Thesis Title THEORETICAL STUDY ON L-PROLINE-CATALYZED
INTRAMOLECULAR CYCLIZATION OF AMINOKETONE
AND ALDEHYDE TO QUINOLINONE DERIVATIVES
By Mr. Parinya Hongtong
Field of study Petrochemistry and Polymer Science
Thesis Advisor Associate Professor Vithaya Ruangpornvisuti, Dr.rer.nat.

Accepted by the Faculty of Science, Chulalongkorn University in
Partial Fulfillment of the Requirements for the Master's Degree

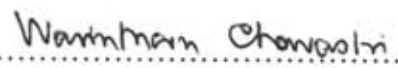

..... Dean of the Faculty of Science
(Professor Supot Hannongbua, Ph.D.)

THESIS COMMITTEE


..... Chairman
(Associate Professor Sirirat Kokpol, Ph.D.)


..... Thesis Advisor
(Associate Professor Vithaya Ruangpornvisuti, Dr.rer.nat.)


..... Member
(Associate Professor Nuanphun Chantarasiri, Ph.D.)


..... Member
(Assistant Professor Dr. Warinthon Chavasiri, Ph.D.)

ปริญญา หงษ์ทอง: การศึกษาเชิงทฤษฎีของการปิดวงแหวนภายในโมเลกุลของแอมิโนคีโตนและแอลดีไฮด์เป็นอนุพันธ์ควิโนลิโนนเร่งปฏิกิริยาด้วยแอล-โพรลีน (THEORETICAL STUDY ON L-PROLINE-CATALYZED INTRAMOLECULAR CYCLIZATION OF AMINOKETONE AND ALDEHYDE TO QUINOLINONE DERIVATIVES) อ. ที่ปรึกษา: รศ.ดร. วิทยา เรืองพรวิสุทธิ์, 63 หน้า

การศึกษากลไกปฏิกิริยาการสังเคราะห์ 2-เอริล-2,3-ไดไฮโดรควิโนลิน-4(1H)-โอิน (P1) และอนุพันธ์ซึ่ง ได้แก่ 2-(4-คลอโร-ฟีนิล)-2,3-ไดไฮโดรควิโนลิน-4(1H)-โอิน (P2) 2-(4-ฟลูออโร-ฟีนิล)-2,3-ไดไฮโดรควิโนลิน-4(1H)-โอิน (P3) และ 2-(4-เมทิล-ฟีนิล)-2,3-ไดไฮโดรควิโนลิน-4(1H)-โอิน (P4) ด้วยการใช้แอล-โพรลีนเป็นตัวเร่งปฏิกิริยา โดยการคำนวณทางเคมีควอนตัมด้วยวิธีเดนซิติฟังก์ชันนัลที่ระดับการคำนวณ B3LYP/6-31G(d) และ B3LYP/6-31+G(d,p) ได้แสดงพลังงานค่าคงที่อัตราการเกิดปฏิกิริยา ค่าคงที่สมดุลของปฏิกิริยาและสมบัติทางเทอร์โมไดนามิกส์ของปฏิกิริยา จากการศึกษาพบว่าปฏิกิริยาการสังเคราะห์ควิโนลิโนน P1, P2, P3 และ P4 เป็นปฏิกิริยาคายพลังงาน กลไกปฏิกิริยาประกอบด้วย 7 ขั้นตอนโดยขั้นที่ 3 ซึ่งมีค่าคงที่อัตราการเกิดปฏิกิริยาเท่ากับ 8.37×10^{-25} , 1.22×10^{-24} , 6.60×10^{-25} และ 9.64×10^{-25} ต่อวินาที ตามลำดับเป็นขั้นกำหนดอัตราการเกิดปฏิกิริยา

สถาบันวิทยบริการ
จุฬาลงกรณ์มหาวิทยาลัย

สาขาวิชา ปิโตรเคมีและวิทยาศาสตร์พอลิเมอร์ ลายมือชื่อนิสิต..... วิทยา หงษ์ทอง
ปีการศึกษา..... 2550..... ลายมือชื่ออาจารย์ที่ปรึกษา.....

4872365823: PETROCHEMISTRY AND POLYMER SCIENCE PROGRAM

KEY WORD: QUINOLINONE/ CYCLIZATION/ L-PROLINE/ DFT

PARINYA HONGTONG: THEORETICAL STUDY ON L-PROLINE-CATALYZED INTRAMOLECULAR CYCLIZATION OF AMINOKETONE AND ALDEHYDE TO QUINOLINONE DERIVATIVES. THESIS ADVISOR: ASSOC. PROF. VITHAYA RUANGPORNVISUTI, Dr.rer.nat., 63 pp.

Mechanisms of synthetic reaction of 2-aryl-2,3-dihydroquinolin-4(1H)-ones (**P1**) and its derivatives, 2-(4-chloro-phenyl)-2,3-dihydroquinolin-4(1H)-one (**P2**), 2-(4-fluoro-phenyl)-2,3-dihydroquinolin-4(1H)-one (**P3**) and 2-(4-methyl-phenyl)-2,3-dihydroquinolin-4(1H)-one (**P4**) catalyzed by L-proline have been investigated using density functional theory method. Energy, rate constants, equilibrium constants and thermodynamic properties for all reaction steps were obtained at the B3LYP/6-31+G(d,p) and B3LYP/6-31G(d) levels of theory. Synthetic reactions for all quinolinone derivatives are an exothermic process and composed of seven reaction steps. Rate determining step of synthetic reactions for products **P1**, **P2**, **P3** and **P4** are their third step and rate constants are 8.37×10^{-25} , 1.22×10^{-24} , 6.60×10^{-25} and $9.64 \times 10^{-25} \text{ s}^{-1}$, respectively.

สถาบันวิทยบริการ
จุฬาลงกรณ์มหาวิทยาลัย

Field of study Petrochemistry and Polymer Science Student's signature พริญา หงตอง
Academic year 2007 Advisor's signature Vithaya Ruangpornvisuti

ACKNOWLEDGEMENTS

I would like to express my sincere gratitude to my advisor Associate Professor Dr. Vithaya Ruangpornvisuti for his continuous attention and guidance throughout the years of my study. I deeply appreciate suggestions and comments of my committee members, Associate Professor Dr. Sirirat Kokpol, Associate Professor Dr. Nuanphun Chantarasiri and Assistant Professor Dr. Warinthon Chavasiri.

The greatest thanks are extended to Mr. Banchob Wano who always assists with intensive quantum and computational chemistry details. Moreover, I greatly appreciated the Petrochemistry and Polymer Science Program and Graduate School Chulalongkorn University for research grant.

Special thanks to all members in Associate Professor Dr. Vithaya Ruangpornvisuti's group for their worthy comments, valuable suggestions and encouragement. I also would like to thank all my friends at Chulalongkorn University for their friendship throughout my study.

Finally, I would like to dedicate this to my parents, for their love, understanding and support for me is priceless.

สถาบันวิทยบริการ
จุฬาลงกรณ์มหาวิทยาลัย

CONTENTS

	Page
ABSTRACT (THAI)	iv
ABSTRACT (ENGLISH)	v
ACKNOWLEDGMENTS	vi
CONTENTS	vii
LIST OF FIGURES	ix
LIST OF TABLES	x
LIST OF ABBRIVIATIONS	xii
CHAPTER I INTRODUCTION	1
1.1 Literature review.....	1
1.2 Scope of research work.....	3
CHAPTER II THEORY	4
2.1 Introduction to Quantum Mechanics.....	4
2.2 Solution of the Schrödinger Equation of Molecular Systems.....	4
2.2.1 The Schrödinger Equation.....	4
2.2.2 Born-Oppenheimer Approximation.....	6
2.3 The Hartree-Fock method.....	7
2.4 Basis Sets.....	9
2.4.1 Minimal Basis Sets.....	11
2.4.2 Scaled Orbital by Splitting the Minimum Basis Sets.....	12
2.4.3 Polarized Basis Sets.....	13
2.4.4 Diffuse Function Basis Sets.....	14
2.5 Density Functional Theory (DFT).....	14
2.6 Transition State Theory and Statistical Mechanics.....	16
2.6.1 Rate constant.....	18
2.7 Thermochemistry.....	19

2.7.1 Partition functions.....	20
CHAPTER III DETAIL OF THE CALCULATION.....	22
3.1 Rate constant.....	22
3.2 Programs used in calculation.....	24
CHAPTER IV RESULTS AND DISCUSSION.....	25
4.1 Reaction mechanism for synthesis of P1.....	26
4.2 Reaction mechanism for synthesis of P2.....	32
4.3 Reaction mechanism for synthesis of P3.....	37
4.4 Reaction mechanism for synthesis of P4.....	42
CHAPTER V CONCLUSION AND SUGGESTION FOR FUTURE WORK	49
REFERENCES.....	51
APPENDIX.....	54
APPENDIX A.....	55
VITA.....	63

สถาบันวิทยบริการ
จุฬาลงกรณ์มหาวิทยาลัย

LIST OF FIGURES

Figure	Page
1.1	2
Synthesis of 2,3-Dihydro-2-phenylquinolone Derivatives 3a-g and Isolation of the intermediate 2-ag.....	
2.1	16
Schematic illustration of reaction path	
2.2	17
The difference between rate constant (<i>k</i>) and equilibrium constant (<i>K</i>).....	
2.3	18
Energy profile E: Potential energy reaction coordinate for A and B via TS [AB] [‡]	
3.1	23
An expected Reaction mechanisms for syntheses of the 2-aryl-2,3-dihydroquinolin-4(1H)-one (P1).....	
4.1	27
Reaction mechanism for synthesis of the 2-aryl-2,3-dihydroquinolin-4(1H)-one, P1.....	
4.2	28
The B3LYP/6-31+G(d,p) optimized structures of transition states in reaction mechanism for synthesis of the 2-aryl-2,3-dihydroquinolin-4(1H)-one, P1.....	
4.3	29
Energy profile for synthesis reaction of the 2-aryl-2,3-dihydroquinolin-4(1H)-one.....	
4.4	32
Reaction mechanism for synthesis of the P2 product.....	
4.5	33
The B3LYP/6-31+G(d,p) optimized structures of transition states in reaction mechanism for synthesis of the P2 product.....	
4.6	34
Energy profile for synthesis reaction of the P2 product.....	
4.7	37
Reaction mechanism for synthesis of the P3 product.....	
4.8	38
The B3LYP/6-31+G(d,p) optimized structures of transition states in reaction mechanism for synthesis of the P3 product.....	
4.9	39
Energy profile for synthesis reaction of the P3 product.....	
4.10	42
Reaction mechanism for synthesis of the P4 product.....	
4.11	43
The B3LYP/6-31+G(d,p) optimized structures of transition states in reaction mechanism for synthesis of the P4 product.....	
4.12	44
Energy profile for synthesis reaction of the P4 product.....	
4.13	46
Mechanism of step 3, nucleophilic substitution of catalyst L-proline and int_2.	

LIST OF TABLES

Table		Page
4.1	Energies, thermodynamic properties, rate constants and equilibrium constants of synthetic reaction of the 2-aryl-2,3-dihydroquinolin-4(1H)-one (P1) catalyzed by L-proline, computed at the B3LYP/6-31+G(d,p) and B3LYP/6-31G(d) (in parenthesis) levels of theory.....	30
4.2	Activation energies, tunneling coefficients, A factors and rate constants of synthetic reaction of 2-aryl-2,3-dihydroquinolin-4(1H)-ones (P1) catalyzed by L-proline, computed at the B3LYP/6-31+G(d,p) and B3LYP/6-31G(d) (in parenthesis) levels of theory.....	31
4.3	Energies, thermodynamic properties, rate constants and equilibrium constants of synthetic reaction of P2 product catalyzed by L-proline, computed at the B3LYP/6-31+G(d,p) and B3LYP/6-31G(d) (in parenthesis) levels of theory.....	35
4.4	Activation energies, tunneling coefficients, A factors and rate constants of synthetic reaction of P2 product catalyzed by L-proline, computed at the B3LYP/6-31+G(d,p) and B3LYP/6-31G(d) (in parenthesis) levels of theory.....	36
4.5	Energies, thermodynamic properties, rate constants and equilibrium constants of synthetic reaction of P3 product catalyzed by L-proline, computed at the B3LYP/6-31+G(d,p) and B3LYP/6-31G(d) (in parenthesis) levels of theory.....	40
4.6	Activation energies, tunneling coefficients, A factors and rate constants of synthetic reaction of P3 product catalyzed by L-proline, computed at the B3LYP/6-31+G(d,p) and B3LYP/6-31G(d) (in parenthesis) levels of theory.....	41
4.7	Energies, thermodynamic properties, rate constants and equilibrium constants of synthetic reaction of P4 product catalyzed by L-proline, computed at the B3LYP/6-31+G(d,p) and B3LYP/6-31G(d) (in parenthesis) levels of theory.....	45

4.8	Activation energies, tunneling coefficients, A factors and rate constants of synthetic reaction of P4 product catalyzed by L-proline, computed at the B3LYP/6-31+G(d,p) and B3LYP/6-31G(d) (in parenthesis) levels of theory.....	46
-----	---	----

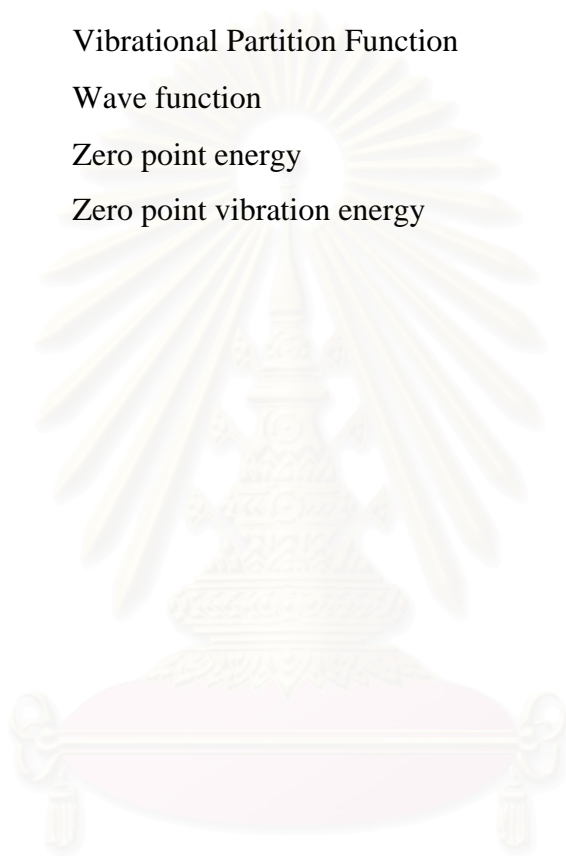


สถาบันวิทยบริการ
จุฬาลงกรณ์มหาวิทยาลัย

LIST OF ABBRIVIATIONS

T	Absolute temperature
ϵ	A diagonal matrix of the orbital energies ϵ_i
\AA	Angstrom
ϕ	Basic function
B3LYP	Becke's three parameters hybrid density functional using the Lee, Yang and Parr correlation functional
k_B	Boltzmann's constant
DFT	Density functional theory
Q^E	Electronic Partition Function
E	Energy
H	Enthalpy
S	Entropy
K	Equilibrium constant
R	Gas constant
GTO	Gaussian type orbital
q	Geometric parameter
G	Gibbs free energy
\hat{H}	Hamiltonian operator
$\tilde{\nu}$	Harmonic vibrational frequency
HF	Hartree–Fock
ν_i	Imaginary Frequency
int	Intermediate
kcal/mol	Kilocalorie per mole
LCAO	Linear combination of atomic orbital
MO	Molecular Orbital
χ	Mulliken electronegativity
Q	Partition function
h	Plank's constant
A	Pre-exponential factor
k	Rate constant

Q^R	Rotational Partition Function
σ	Rotational symmetry number of the molecule
STO	Slater type orbital
c	Speed of light
TS	Transition state
TST	Transition state theory
Q^T	Translational Partition Function
Q^V	Vibrational Partition Function
ψ	Wave function
ZPE	Zero point energy
ZPVE	Zero point vibration energy



สถาบันวิทยบริการ
จุฬาลงกรณ์มหาวิทยาลัย

CHAPTER I

INTRODUCTION

Cyclization reaction is one of importance reaction in petrochemical industry, especially in production of chemicals for industrial use. Some chemicals that produced from the cyclization reaction are indoles, chalcones, quinolines, benzimidazoles, benzotriazoles, indazoles, tetrahydrofuran and etc [1,2]. In this work we study on intramolecular cyclization of aminoketone and aldehyde to form quinolinone and its derivatives catalyzed by L-proline. This product quinolinone can be applied in agricultural industrial [3] as fungicides, insecticides and herbicides. In cosmetic [4], paint and paper production quinolinone are also use as bactericides in industrial applications [5], for example in waterbased paint and in the white water of paper mills to inhibit the growth of harmful bacteria.

1.1 Literature review

For the past years there are a lot of research in cyclization reaction. The involved examples are given as follow.

In 1999 Arcadia *et al.* [6] studied on synthesis of quinoline by nucleophilic addition reaction. The reactions were generally carried out at 60-80 °C, in the presence of an excess of nucleophile or pronucleophile and the 2,4-disubstituted quinolines 3 were isolated in good yields as sole products through a conjugate addition/cyclization reaction.

In 2001 Wang *et al.* [7] investigated in the reaction of a α -aroylketene dithioacetals with esters of *o*-aminobenzoic acid under different conditions afforded preferentially 2-methylthio-3-aroylquinolones and 2-anilino-3-aroylquinolines through, respectively, α -aroylketene *N,S*-acetal and α -aroylketene aiminal intermediates. The annulation reaction of 2-methylthio-3-aroylquinolones with hydrazine gave both pyrazolo[3,4-*b*]quinolone and pyrazolo[4,3-*c*]quinoline, the selectivity being determined by the reaction conditions employed. Intramolecular cyclocondensation of 2-anilino-3-aroylquinolines produced quino[2,1-*b*]quinazolines in high yield. We therefore envisaged that a tandem reaction comprising the formation

of ketene amins between α -aroylketene dithioacetals and *o*-aminobenzoic acid esters followed by an intramolecular enaminic cyclization would furnish quinolines or quinolones.

In 2003 Bahmanyar *et al.* [8] reported that quantum mechanical calculations were employed to predict the ratio of four stereoisomeric products expected from two complex reactions involving the aldol reactions of cyclohexanone with benzaldehyde or with isobutyraldehyde catalyzed by (S)-proline. Experimental tests of these predictions provide an assessment of the state-of-the-art in quantum mechanical prediction of products of complex organic reactions in solution.

Stationary points (reactant and transition state geometries) were optimized and characterized by frequency analysis using hybrid density functional theory (B3LYP) and the 6-31G basis set as implemented in Gaussian 98.

In 2004 Park *et al.* [9] reported that A series of 2,3-dihydro-2-phenyl-4-quinolones **3a-g** has been synthesized using acid-catalyzed one-pot reaction. (Figure 1.1) Quinolones **3a-g** were prepared through cyclization of the condensation product **2a-g** that were formed by heating of arylamines and ethyl benzoylacetate in toluene. Similarly, the 6 (7 or 8)-substituted 2,3-dihydro-2-phenylquinolones were prepared from the para(ortho or meta)-substituted aniline. The reaction mechanism of the formation of the final product involves the nucleophilic dehydration and following cyclization between arylamines and ethyl benzoylacetate (EBA). Nucleophilic dehydration, the condensation was undertaken with *p*-toluene sulfonic acid at 90-110 °C in toluene for 2-6 hours over the dean- stark apparatus for the ester **2**. The ester **2** was continuously converted to the 2-phenylquinolones **3** with removal of ethanol and dihydrogenation. All synthetic process from arylamines and ethyl benzoylacetate to quinolones **3a-g** could be carried out in one-pot without isolation of intermediates.

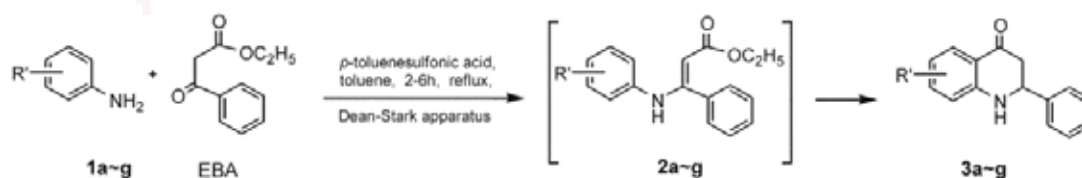


Figure 1.1 Synthesis of 2,3-Dihydro-2-phenylquinolone Derivatives **3a-g** and Isolation of the intermediate **2a-g**.

In 2005 Sabitha *et al.* [10] reported that D,L-Proline was found to catalyze efficiently the one-pot trimolecular condensation of indoles, a sugar hydroxyaldehyde, and Meldrum's acid (2,2-dimethyl-1,3-dioxane-4,6-dione) followed by intramolecular cyclization with evolution of carbon dioxide and elimination of acetone to afford 7-(1H-3-indolyl)-2,3-dimethoxyperhydrofuro[3,2-b]pyran-5-ones. The reaction proceeded cleanly at ambient temperature to afford the products in good yields with high diastereoselectivity.

In 2005 Chandrasekhar *et al.* [11] reported that L-Proline is utilized as an organocatalyst for the synthesis of substituted 2-aryl-2,3-dihydroquinolin-4(1H)-ones, in good yields. The efficiency of the catalyst was proved with a variety of substrates ranging from electron-deficient to electron-rich aryl aldehydes. We demonstrated that 2-hydroxyacetophenones and aryl aldehydes undergo a smooth one-pot condensation cyclization in the presence of L-proline as organocatalyst to furnish flavanones in high yields.

In 2007 Lee *et al.* [2] reported that A series of β -bromo- and β -iodotetrahydrofurans was synthesized from the reaction mixture of 5-hydroxypentene, L-proline, NBS (or I₂) in THF at 0 °C for 10 min. This L-proline-catalyzed intramolecular cyclization provides a simple and efficient method for the preparation of β -halogenated tetrahydrofuran.

1.2 Scope of research work

This work study on reaction mechanism of synthetic reaction of quinolinones and its derivatives. We have study on 4 different substituents of reactant benzaldehyde to synthesis 4 quinolinone derivatives, reactant benzaldehyde are substituted by H (benzaldehyde), Cl (*p*-chlorobenzaldehyde), F (*p*-fluorobenzaldehyde) and CH₃ (*p*-methylbenzaldehyde).

CHAPTER II

THEORETICAL BACKGROUND

2.1 Introduction to Quantum Mechanics

The word quantum comes from Latin (quantum, “how much?”) and is first used by Max Plank in 1900 to denote the constrained quantities or amounts in which energy can be emitted or absorbed. “Mechanics” as used in physics is traditionally the study of the behavior of bodies under the action of forces. The term “quantum mechanics” is apparently first used by Born (of the Born-Oppenheimer approximation) in 1924. Because molecules are consisted of nuclei and electrons, quantum chemistry deals with the motion of electrons under the influence of the electromagnetic force exerted by nuclear charges. An understanding of the behavior of electrons in molecules, structures and reactions of molecules, rest on quantum mechanics and in particular on the adornment of quantum chemistry, the Schrödinger equation [12].

2.2 Solution of the Schrödinger Equation of Molecular Systems

2.2.1 The Schrödinger Equation

The ultimate goal of most quantum chemical approaches is the approximate solution of the time-independent, non-relativistic Schrödinger equation:

$$\hat{H}\psi_i(\vec{x}_1, \vec{x}_2, \dots, \vec{x}_N, \vec{R}_1, \vec{R}_2, \dots, \vec{R}_M) = E_i \psi_i(\vec{x}_1, \vec{x}_2, \dots, \vec{x}_N, \vec{R}_1, \vec{R}_2, \dots, \vec{R}_M) \quad (2.1)$$

where \hat{H} is the Hamilton operator for a molecular system consisting of M nuclei and N electrons in the absence of magnetic or electric fields. \hat{H} is a differential operator representing the total energy:

$$\hat{H} = -\frac{1}{2} \sum_{i=1}^N \nabla_i^2 - \frac{1}{2} \sum_{A=1}^M \frac{1}{M_A} \nabla_A^2 - \sum_{i=1}^N \sum_{A=1}^M \frac{Z_A}{r_{iA}} + \sum_{i=1}^N \sum_{j>i}^N \frac{1}{r_{ij}} + \sum_{A=1}^M \sum_{B>A}^M \frac{Z_A Z_B}{R_{AB}} \quad (2.2)$$

Here, A and B run over the M nuclei while i and j denote the N electrons in the system. The first two terms describe the kinetic energy of the electrons and nuclei respectively, where the Laplacian operator ∇_q^2 is defined as a sum of differential operators (in cartesian coordinates):

$$\nabla_q^2 = \frac{\partial^2}{\partial x_q^2} + \frac{\partial^2}{\partial y_q^2} + \frac{\partial^2}{\partial z_q^2} \quad (2.3)$$

M_A is the mass of nucleus A in multiples of the mass of an electron. The remaining three terms define the potential parts of the Hamiltonian and represent the attractive electrostatic interaction between the nuclei and the electrons and the repulsive potential due to electron-electron and nucleus-nucleus interactions, respectively. R_{pq} (and similarly R_{qp}) is the distance between the particles p and q, i.e., $r_{pq} = |\vec{r}_p - \vec{r}_q|$. $\Psi_i(\vec{x}_1, \vec{x}_2, \dots, \vec{x}_N, \vec{R}_1, \vec{R}_2, \dots, \vec{R}_M)$ stands for the wave function of the i^{th} state of the system, which depends on the $3N$ spatial coordinates $\{\vec{r}_i\}$, and the N spin coordinates $\{S_i\}$ of the electrons, which are collectively termed $\{\vec{x}_i\}$, and the $3M$ spatial coordinates of the nuclei, $\{\vec{R}_I\}$. The wave function Ψ_i contains all information that can possibly be known about the quantum system at hand. Finally, E_i is the numerical value of the energy of the state described by Ψ_i .

All equations given in this text appear in a very compact form, without any fundamental physical constants. We achieve this by employing the so-called system of atomic units, which is particularly adapted for working with the atoms and molecules. In this system, physical quantities are expressed as multiples of fundamental constants and, if necessary, as combinations of such constants. The mass of an electron, m_e , the modulus of its charge, $|e|$, Planck's constant h divided by 2π , \hbar , and $4\pi\epsilon_0$, the permittivity of the vacuum, are all set to unity. Mass, charge, action etc. are then expressed as multiples of these constants, which can therefore be dropped from all equations [12].

2.2.2 Born-Oppenheimer Approximation

The Schrödinger equation can be further simplified if we take advantage of the significant differences between the masses of nuclei and electrons. Even the lightest of all nuclei, the proton (${}^1\text{H}$), weighs roughly 1800 times more than an electron. Thus, the nuclei move much slower than the electrons. The practical consequence is that we can at least to a good approximation take the extreme point of view and consider the electrons as moving in the field of fixed nuclei. This is the famous *Born-Oppenheimer* or clamped-nuclei approximation. If the nuclei are fixed in space and do not move, their kinetic energy is zero and the potential energy due to nucleus-nucleus repulsion is merely a constant. Thus, the complete Hamiltonian given in equation (2.4) reduces to the so-called electronic Hamiltonian:

$$\hat{H}_{elec} = \frac{1}{2} \sum_{i=1}^n \nabla_i^2 - \sum_{i=1}^n \nabla_i^2 \sum_{A=1}^K \frac{Z_A}{r_{iA}} + \sum_{i=1}^n \sum_{j>1}^n \frac{1}{r_{ij}} \quad (2.4)$$

The solution of the Schrödinger equation with \hat{H}_{elec} is the electronic wave function ψ_{elec} and the electronic energy E_{elec} . ψ_{elec} depends on the electron coordinates, while the nuclear coordinates enter only parametrically and do not explicitly appear in ψ_{elec} . The total energy E_{tot} is then the sum of E_{elec} and the constant nuclear repulsion term [13]:

$$E_{nuc} = \sum_{A=1}^K \sum_{B>A}^M \frac{Z_A Z_B}{r_{AB}} \quad (2.5)$$

$$\hat{H}_{elec} \psi_{elec} = E_{elec} \psi_{elec} \quad (2.6)$$

and

$$E_{tot} = E_{elec} + E_{nuc} \quad (2.7)$$

The attractive potential exerted on the electrons due to the nuclei – the expectation value of the second operator \widehat{V}_{Ne} in equation (2.4) is often termed the external potential, V_{ext} , in density functional theory, even though the external potential is not necessarily limited to the nuclear field but may include external magnetic or electric fields etc. From now on we will only consider the electronic problem of equations (2.4)-(2.6) and the subscript “elec” will be dropped.

2.3 The Hartree-Fock Method

The Hartree-Fock method seeks to approximately solve the electronic Schrödinger equation, and it assumes that the wave function can be approximated by a single Slater determinant made up of one spin orbital per electron. Since the energy expression is symmetric, the variation theorem holds, and so we know that the Slater determinant with the lowest energy is as close as we can get to the true wave function for the assumed functional form of a single Slater determinant. The Hartree-Fock method determines the set of spin orbitals which minimize the energy and give us this best single determinant. So, we need to minimize the Hartree-Fock energy expression with respect to changes in the orbitals:

$$\chi_i \rightarrow \chi_i + \delta \chi_i \quad (2.8)$$

We have also been assuming that the orbitals are orthonormal, and we want to ensure that our variational procedure leaves them orthonormal. The Hartree-Fock equations can be solved numerically (exact Hartree-Fock), or they can be solved in the space spanned by a set of basis functions (Hartree-Fock-Roothan equations). In either case, note that the solutions depend on the orbitals. Hence, we need to guess some initial orbitals and then refine our guesses iteratively. For this reason, Hartree-Fock is called a *self-consistent-field* (SCF) approach.

The first term above in square brackets:

$$\sum_{j \neq i} \left[\int dx_2 |\chi_j(x_2)|^2 r_{12}^{-1} \right] \chi_i(x_1), \quad (2.9)$$

gives the Coulomb interaction of an electron in spin orbital χ_i with the average charge distribution of the other electrons. Here we see in what sense Hartree-Fock is a mean field theory. This is called the *Coulomb term*, and it is convenient to define a Coulomb operator as:

$$J_j(x_1) = \int dx_2 |\chi_j(x_2)|^2 r_{12}^{-1}, \quad (2.10)$$

which gives the average local potential at point x_1 due to the charge distribution from the electron in orbital χ_j .

We can define an exchange operator in terms of its action on an arbitrary spin orbital χ_i :

$$K_j(x_1)\chi_i(x_1) = \left[\int dx_2 \chi_j^*(x_2) r_{12}^{-1} \chi_i(x_2) \right] \chi_j(x_1). \quad (2.11)$$

Introducing a basis set transforms the Hartree-Fock equations into the Roothaan equations. Denoting the atomic orbital basis functions as $\bar{\chi}$, we have the expansion:

$$\chi_i = \sum_{\mu=1}^K C_{\mu i} \bar{\chi}_{\mu} \quad (2.12)$$

for each spin orbital χ_i . This leads to:

$$f(x_1) \sum_v C_{vi} \tilde{\chi}_v(x_1) = \epsilon_i \sum_v C_{vi} \tilde{\chi}_v(x_1). \quad (2.13)$$

This can be simplified by introducing the matrix element notation :

$$S_{\mu\nu} = \int dx_1 \bar{\chi}_{\mu}^*(x_1) \bar{\chi}_{\nu}(x_1), \quad (2.14)$$

$$F_{\mu\nu} = \int dx_1 \bar{\chi}_{\mu}^*(x_1) \bar{\chi}_{\nu}(x_1). \quad (2.15)$$

Now the Hartree-Fock-Roothaan equations can be written in matrix form as:

$$\sum_{\nu} F_{\mu\nu} C_{\nu i} = \epsilon_i \sum_{\nu} S_{\mu\nu} C_{\nu i} \quad (2.16)$$

or even more simply as matrices:

$$FC = SC\epsilon \quad (2.17)$$

where ϵ is a diagonal matrix of the orbital energies ϵ_i . This is like an eigenvalue equation except for the overlap matrix S . One performs a transformation of basis to go to an orthogonal basis to make S vanish. Then it's just a matter of solving an eigenvalue equation. Well, not quite. Since F depends on its own solution (through the orbitals), the process must be done iteratively. This is why the solution of the Hartree-Fock-Roothaan equations are often called the self-consistent-field procedure [13].

2.4 Basis Sets

The approximate treatment of electron-electron distribution and motion assigns individual electrons to one-electron function, termed *spin orbital*. These consist of a product of spatial functions, termed *molecular orbitals (MO)*, $\psi_1(x, y, z)$, $\psi_2(x, y, z)$, $\psi_3(x, y, z)$, ..., and either α or β spin components. The spin orbitals are allowed complete freedom to spread throughout the molecule. Their exact forms are determined to minimize the total energy. In the simplest level of theory, a single assignment of electron to orbital is made by using ψ as atomic orbital wave function based on the Schrödinger equation for the hydrogen atom. This is not a suitable approach for molecular calculation. This problem can be solved by representing MO as linear combination of basis functions.

In practical calculation, the molecular orbitals ψ_1, ψ_2, \dots , are further restricted to be linear combinations of a set of N known one-electron function $\phi_1(x, y, z), \phi_2(x, y, z), \dots, \phi_N(x, y, z)$:

$$\psi_i = \sum_{\mu=1}^N c_{\mu i} \phi_{\mu} \quad (2.18)$$

The functions $\phi_1, \phi_2, \dots, \phi_N$, which are defined in the specification of the model, are known as one-electron basis function called basis function. The set of basis functions is called basis set. If the basis functions are the atomic orbitals for the atoms making up the molecule, function in equation 2.18 is often described as the *linear combination of atomic orbitals* (LCAO). There are two types of basis function which commonly used in the electronic structure calculations, *Slater type orbitals* (STO) and *Gaussian type orbitals* (GTO).

The Slater orbitals are primarily used for atomic and diatomic systems where high accuracy is required and semiempirical calculations where all three- and four-center integrals are neglected. The Slater type orbitals have the function form:

$$b = A e^{-\zeta r} r^{n^*-1} Y_{lm}(\theta, \phi) \quad (2.19)$$

where parameter n^* and ζ are chosen to make the larger part of the orbitals look like atomic Hartree-Fock orbitals. There are a lot like hydrogen orbitals, but without the complicated nodal structure.

The Gaussian type orbitals can be written in terms of polar or cartesian coordinates:

$$g = x^a y^b z^c e^{-\alpha r^2} Y_{lm}(\theta, \phi) \quad (2.20)$$

in which a, b , and c are integers and α is a parameter that is usually fixed. Primitive Gaussian function is shown in equation 2.20. Normally, several of these Gaussian

functions are summed to define more realistic atomic orbitals basis functions, as shown below:

$$b_{\mu} = \sum_p k_{\mu p} g_p. \quad (2.21)$$

The coefficients $k_{\mu p}$ in this expansion are chosen to make the basis functions look as much like Slater orbitals as possible. Slater functions are good approximation to atomic wave functions but required excessive computer time more than Gaussian functions, while single-Gaussian functions are a poor approximation to the nearly ideal description of an atomic wave function that Slater function provides. The solution to the problem of this poor functional behavior is to use several Gaussians to approximate a Slater function. In the simplest version of this basis, n Gaussian functions are superimposed with fixed coefficients to form one-Slater type orbital. Such a basis is denoted STO-nG, and $n = 3, 4$.

The limit of quantum mechanics involves an infinite set of basis function. This is clearly impractical since the computational expanse of molecular orbital calculations is proportional to the power of the total number of basis functions. Therefore, ultimate choice of basis set size demands on a compromise between accuracy and efficiency. The classification of basis sets is given below.

2.4.1 Minimal Basis Sets

The minimum basis set is a selected basis function for every atomic orbital that is required to describe the free atom. For hydrogen atom, the minimum basis set is just one $1s$ orbital. But for carbon atom, the minimum basis set consisted of a $1s$ orbital, a $2s$ orbital and the full set of three $2p$ orbitals. For example, the minimum basis set for the methane molecule consists of 4 $1s$ orbitals, one per hydrogen atom, and the set of $1s$, $2s$ and $2p$ orbitals described above for carbon. Thus, total basis set comprises of 9 basis functions.

Several minimum basis sets are used as common basis sets especially the STO-nG basis sets because they are available for almost all elements in the periodic table. The

most common of minimum basis sets is STO-3G, where a linear combination of three Gaussian type orbitals (GTOs) is fitted to a Slater-type orbital (STO). The individual GTOs are called primitive orbitals, while the combined functions are called contracted functions. For example, the STO-3G basis set for methane consists of a total of 9 contracted functions built from 27 primitive functions. Other commonly used STO-nG basis sets are STO-4G and STO-6G where each STO is fitted to 4 and 6 GTOs, respectively.

2.4.2 Scaled Orbital by Splitting the Minimum Basis Sets

In the early calculation on the hydrogen molecule, it is discovered that the STO $1s$ orbitals do not give the best result in the molecular environment when the Schrödinger equation is solved, because electron is attracted to both nuclei rather than just one nucleus. In each molecular orbital, both large and small sets of orbital appear and they are mixed in the ratio that gives the lowest energy. The combination of a large orbital and a small orbital is essentially equivalent to an orbital of intermediate size. The result orbital is a size that best fit for the molecular environment since it is obtained from minimizing the energy. The advantage of this procedure is that the mixing coefficients in the molecular orbitals appear in a linear function. This simple dodge is equivalent to scaling the single minimal basis set orbitals. The minimum basis set can scaled not only the valence orbitals of the minimal basis set (split valence basis set), but also all the orbitals of the minimal basis set (double zeta basis sets).

a) Split the Valence Orbitals (Split Valence Basis Sets)

The split valence basis sets mean that each valence orbital is split into two parts, an inner shell and an outer shell. For example, the 3-21G basis set is referred to basis function of the inner shell represented by two Gaussian functions and that of the outer shell represented by one Gaussian function. The core orbitals are represented by one basis function and each function composes of three Gaussian functions. The purpose of splitting the valence shell is to give the SCF algorithm more flexibility in adjusting the

contributions of the basis function to the molecular orbitals, achieving a more realistic simulated electron distribution.

b) Split all Orbitals (Double Zeta Basis Sets)

Double zeta basis set is a member of minimum basis set replaced by two functions. In this way both core and valence orbitals are scaled in size. For some heavier atoms, double zeta basis sets may have slightly less than double the number of minimum basis set orbitals. For example, some double zeta basis sets for the atoms Ga-Br have 7 rather than 8 *s* basis functions, and 5 rather than 6 *p* basis functions.

The term “*double zeta*” arises from the fact that the exponent in a STO is often referred by the Greek letter “*zeta*”. Since it takes two orbitals with different exponents, it is called “*double zeta*”. The minimum basis set is “*single zeta*”. The normal abbreviation for a double zeta basis set is DZ. It is also quite common to use split valence basis sets where the valence orbitals are spitted into three functions. Basis sets where this is done for all functions are called triple zeta functions and referred to as TZ, TZP, TZ2P etc.

2.4.3 Polarized Basis Sets

In the discussion on the scaling of the hydrogen orbitals in the H₂ molecule, it is argued that the orbital on one atom in the molecule becomes smaller because of the attraction of the other nucleus. However, it is also clear that the influence of the other nucleus may distort or polarize the electron density near the nucleus. This problem desires orbitals that have more flexible shapes in a molecule than the *s*, *p*, *d*, etc., shapes in the free atoms. This is best accomplished by add basis functions of higher angular momentum quantum number. Thus, the spherical *1s* orbital on hydrogen is distorted by mixing in an orbital with *p* symmetry. The positive lobe at one side increases the value of the orbital while the negative lobe at the other side decreases the orbital. The orbital has overall “moved” sideways. It has been polarized. Similarly, the *p* orbital can polarize if it mixes in an orbital of *d* symmetry. These additional basis functions are called polarization functions. The polarization functions are added to the 6-31G basis set as follows:

6-31G* added a set of d orbitals to the atoms in the first and second rows .

6-31G** added a set of d orbitals to the atoms in the first and second rows and a set of p functions to hydrogen.

The nomenclature above is slowly being replaced. The 6-31G* is called 6-31G(d), while the 6-31G** is called 6-31G(d,p). This new nomenclature allows the possibility of adding several polarization functions. Thus 6-31G (3df,pd) added 3 d -type GTOs and 1 f -type GTO and added 1 p -type and 1 d -type function to H.

2.4.4 Diffuse Function Basis Sets

In some cases the normal basis functions are not adequate. This is particular the case in excited states and in anions where the electronic density is spread out more over the molecule. This model has correctly by using some basis functions which themselves are more spread out. This means that small exponents are added to GTOs. These additional basis functions are called diffuse functions. The diffuse functions added to the 6-31G basis set as follows:

6-31+G added a set of diffuse s and p orbitals to the atoms in the first and second rows.

Diffuse functions can be added along with polarization functions also. Some examples of these functions are 6-31+G*, 6-31++G*, 6-31+G** and 6-31++G** basis sets.

2.5 Density Functional Theory (DFT)

The ab initio methods described The basis for Density Functional Theory (DFT) is the proof by Hohenberg and Kohn that the ground-state electronic energy is determined completely by the electron density ρ . In other words, there exists a one-to-one correspondence between the electron density of a system and the energy. The significance of this is perhaps best illustrated by comparing to the wave function approach. A wave function for an N -electron system contains $3N$ coordinates, three for each electron (four if spin is included). The electron density is the square of the wave function, integrated over $N-1$ electron coordinates, this only depends on three

coordinates, independently of the number of electrons. While the complexity of a wave function increases with the number of electrons, the electron density has the same number of variables, independently of the system size. The “only” problem is that although it has been proven that each different density yields a different ground-state energy, the functional connection these two quantities is not known. The goal of DFT methods is to design functionals connecting the electron density with the energy.

The foundation for the use of DFT methods in computational chemistry was the introduction of orbitals by Kohn and Sham. The basic idea in the Kohn and Sham (KS) formalism is splitting the kinetic energy functional into two parts, one of which can be calculated exactly, and a small correction term.

The key to Kohn-Sham theory is thus the calculation of the kinetic energy under the assumption of non-interacting electrons. In reality the electrons are interacting, and equation (2.22) does not provide the total kinetic energy. The remaining kinetic energy is absorbed into an exchange – correlation term, and a general DFT energy expression can be written as

$$E_{DFT}[p] = T_S[p] + E_{ne}[p] + J[p] + E_{xc}[p] \quad (2.22)$$

By equating E_{DFT} to the exact energy E_{xc} , it is the part which remains after subtraction of the non-interacting kinetic energy, and the E_{ne} and J potential energy terms:

$$E_{xc}[p] = (T[p] - T_S[p]) + (E_{ee}[p] - J[p]) \quad (2.23)$$

The first parenthesis in equation (2.23) may be considered the kinetic correlation energy, while the second contains both exchange and potential correlation energy [17].

2.6 Transition State Theory and Statistical Mechanics

Transition state theory (TST) assumes that a reaction proceeded from one energy minimum to another *via* an intermediate maximum. The *transition state* is the configuration which divides the reactant and product parts of surface. For example, a molecule which has reached the transition state is continuing to product. The geometrical configuration of the energy maximum is called the *transition structure*. Within standard TST, the transition state and transition structure are identical, but this is not necessarily for more refined models. The direction of reaction coordinate is started from the reactant to product along a path where the energies are as low as possible and the TS is the point where the energy has a maximum. In the multidimensional case, TS is a first-order point on the potential energy surface as a maximum in the reaction coordinate direction and a minimum along all other coordinates, shown in Figure 2.1.

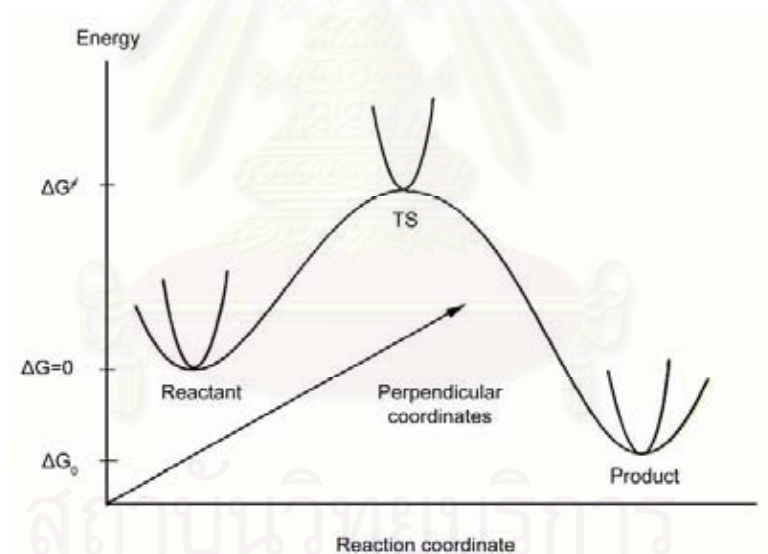


Figure 2.1 Schematic illustration of reaction path [13].

Transition state theory assumes equilibrium energy distribution among all possible quantum states at all points along the reaction coordinates. The probability of finding a molecule in a given quantum state is proportional to $e^{-\Delta E/k_B T}$, which is

Boltzman distribution. Assuming that the molecule at the TS is in equilibrium with the reactant, the macroscopic rate constant can be expressed as:

$$k = \frac{k_B T e^{-\Delta G^\ddagger / RT}}{h} \quad (2.24)$$

in which ΔG^\ddagger is the Gibbs free energy difference between the TS and reactant, T is absolute temperature and k_B is Boltzmann's constant. It is clear that if the free energy of the reactant and TS can be calculated, the reactant rate follows trivially. The equilibrium constant for a reaction can be calculated from the free energy difference between the reactant and product.

$$K_{eq} = e^{-\Delta G_0 / RT} \quad (2.25)$$

The Gibbs free energy is given in terms of the enthalpy and entropy, $G = H - TS$. The enthalpy and entropy for a macroscopic ensemble of particles maybe calculated from properties of the individual molecules by means of statistical mechanics.

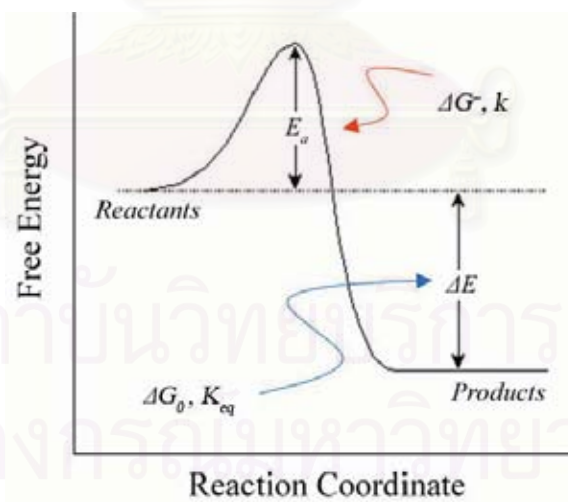
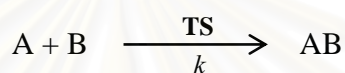


Figure 2.2 The difference between rate constant (k) and equilibrium constant (K) [13].

2.6.1 Rate constant

An activated complex AB^\ddagger or transition state is formed at the potential energy maximum as shown in Figure 2.3. The high-energy complex represents an unstable molecular arrangement, in which bonds break and form to generate the product AB or to degenerate back to the reactants A and B as shown in equation 2.26. In the simple form of transition state theory, it is supposed that the transition state (TS) is in equilibrium with the reactants, and that its abundance in the reaction mixture can be expressed in terms of an equilibrium constants, which is normally denoted K :



$$K = \frac{[AB]}{[A][B]} \quad (2.26)$$

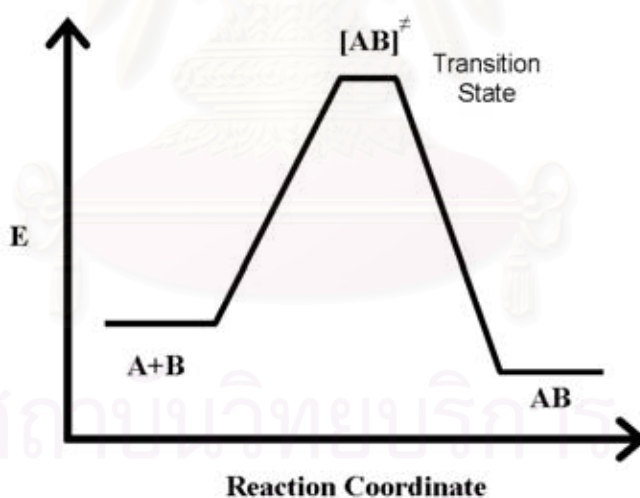


Figure 2.3 Energy profile E: Potential energy reaction coordinate for A and B via TS $[AB]^\ddagger$.

Then, if we supposed that the rate at which products are formed is proportional to the concentration of the TS, we can write

rate of formation of products = $k[\text{TS}]$

We see that the rate constant k is proportional to the equilibrium constants K^\ddagger for the formation of the TS. We have already seen that an equilibrium constant may be expressed in terms of the standard reaction Gibbs energy, which in this case is the activation Gibbs energy, $\Delta^\ddagger G$, for the formation of the TS from the reactants. It follows from the equation 2.26 that

$$K = e^{-\Delta^\ddagger G / RT} \quad (2.27)$$

Furthermore $\Delta^\ddagger G$ is given by

$$\Delta^\ddagger G = \Delta^\ddagger H - T\Delta^\ddagger S \quad (2.28)$$

Combining equation 2.27 and the equation 2.28 and solving for $\ln k$ yields

$$\ln K = \frac{-\Delta^\ddagger H}{RT} + \frac{-\Delta^\ddagger S}{R} \quad (2.29)$$

The *Eyring equation*: is found by substituting equation 2.29 into equation 2.27

$$k = \frac{k_B T}{h} e^{\frac{\Delta^\ddagger H}{RT}} e^{\frac{\Delta^\ddagger S}{R}} \quad \text{or} \quad k = \frac{k_B T}{h} e^{\frac{-\Delta^\ddagger G}{RT}} \quad (2.30)$$

2.7 Thermochemistry

The term energy in chemistry can mean potential energy, enthalpy, or Gibbs energy. The potential energy on a computed Born-Oppenheimer surface represents 0K enthalpy difference without ZPE. Enthalpy difference ΔH and free energy difference ΔG are related through the entropy difference:

$$\Delta G = \Delta H - T \Delta S \quad (2.31)$$

To get an intuitive feel for ΔH , ΔG and ΔS we can regard it as essentially measure of the reaction enthalpy between product and reactant:

$$\Delta H = H_{\text{product}} - H_{\text{reactant}} \quad (2.32)$$

$$\Delta G = G_{\text{product}} - G_{\text{reactant}} \quad (2.33)$$

$$\Delta S = S_{\text{product}} - S_{\text{reactant}} \quad (2.34)$$

2.7.1 Partition functions

The first step in determining the thermal contributions to the enthalpies and entropies of a molecule is to determine its partition function, Q which is a measure of the number of accessible states to the molecule (translational, rotational, vibrational and electronic states) at a particular temperature.

When given the energies E_i of the available quantum states of a molecule, Q is defined as:

$$Q = \sum_{i=1}^{\infty} g_i e^{-\beta E_i} \quad (2.35)$$

Where g_i is the degeneracy of the i^{th} state and $\beta = \frac{1}{k_B T}$

Where k_B is Boltzmann's constant and T is the temperature of interest. The summation in Equation 2.35 is over all possible quantum states of the system.

It is assumed that the translational (T), rotational (R), vibrational (V) and electronic (E) modes of the system can be separated, thus allowing the energy of each level, E_i , to be separated into T , R , V and E contributions as

$$E = E_i^T + E_i^R + E_i^V + E_i^E \quad (2.36)$$

While the translational modes are truly independent from the rest, the separations of other modes are based on an approximation, in particular the Born–Oppenheimer approximation for electronic and vibrational motion and the rigid rotor approximation which assumes (that the geometry of the molecule does not change as it rotates) for vibrational and rotational modes. Within these approximations, the total molecular partition function can therefore be factorized into translational, rotational, vibrational and electronic contributions:

$$Q = Q^T Q^R Q^V Q^E \quad (2.37)$$

The translational partition function is given by:

$$Q^T = \frac{V}{\Lambda^3} \quad (2.38)$$

$$\Lambda = h \left(\frac{\beta}{2\pi m} \right)^{1/2} \quad (2.39)$$

Where h is Planck's constants, m is the mass of the molecule and V is the available volume to it. For a gas phase system this is the molar volume (usually determined by the ideal gas equation) at the specific temperature and pressure.

The formulation for rotational partition functions depends on whether or not the molecule is linear. For linear molecules

$$Q^R = \frac{k_B T}{\sigma h c B} \quad (2.40)$$

and for non linear

$$Q^R = \frac{1}{\sigma} \left(\frac{k_B T}{h c} \right)^{3/2} \left(\frac{\pi}{ABC} \right)^{1/2} \quad (2.41)$$

Where σ is the rotational symmetry number of the molecule, c is the speed of light and A , B , C are the rotational constants. The vibrational partition function in the harmonic approximation is

$$Q^V = \prod_i \frac{1}{1 - e^{-\beta h c \tilde{\nu}_i}} \quad (2.42)$$

Where $\tilde{\nu}$ is the harmonic vibrational frequencies (expressed as wave numbers) and the product is taken over all ($3N-6$ or $3N-5$) vibrational modes (excluding the reaction coordinate for transition states). For the electronic partition function it is usually assumed that there is no thermal excitation into the higher electronic states. Then the partition function, Q^E , is simply given by the degeneracy of the appropriate electronic state.

สถาบันวิทยบริการ
จุฬาลงกรณ์มหาวิทยาลัย

CHAPTER III

DETAIL OF THE CALCULATIONS

The geometry optimizations for all involved species as show in Figure 3.1 were carried out using density function theory (DFT) method [15,16]. The DFT computations have been performed with Becke's three parameters hybrid density functional [17,18] using the Lee, Yang and Parr correlation functional (B3LYP) [19]. The B3LYP/6-31+G(d,p) and B3LYP/6-31G(d) level of calculation has been employed for all geometry optimizations and their thermodynamic properties were derived from the vibrational frequency calculations.

3.1 Rate constant

The standard enthalpy ΔH° and Gibbs free energy changes ΔG° of conversion reactions of this system have been derived from the frequency calculations. Each reaction entropy ΔS° was calculated using a thermodynamic relation of $\Delta S^\circ = (\Delta H^\circ - \Delta G^\circ)/T$. The rate constant $k(T)$, rate constant in term of partition function (k) and equilibrium constant K derived from transition state theory was computed from activation free energy, $\Delta^\ddagger G^\circ$ by equation:

$$k(T) = \frac{k_B T}{hc^\circ} e^{(-\Delta^\ddagger G^\circ/RT)} \quad (3.1)$$

$$k = \kappa \left[\frac{k_B T}{h} \right] \left[\frac{Q_{TS}}{Q_{REA}} \right] e^{(-\Delta^\ddagger E /RT)} \quad (3.2)$$

and

$$K_{eq} = e^{-\Delta G_0 / RT} \quad (3.3)$$

Where concentration factor, c° of unity is used, k_B is Boltzmann's constant, h is Plank's constant, T is the absolute temperature and R is gas constant. The above formula was employed to compute the reaction rate constants for corresponding activation free energies.

In this work we study in 4 difference subsituents. For synthesis 4 quinolinone derivatives, substituent on para-position (H) of benzaldehyde was replaced with Cl, F and CH_3 .

All minima and transition states were confirmed by real and single imaginary vibrational frequencies, respectively.

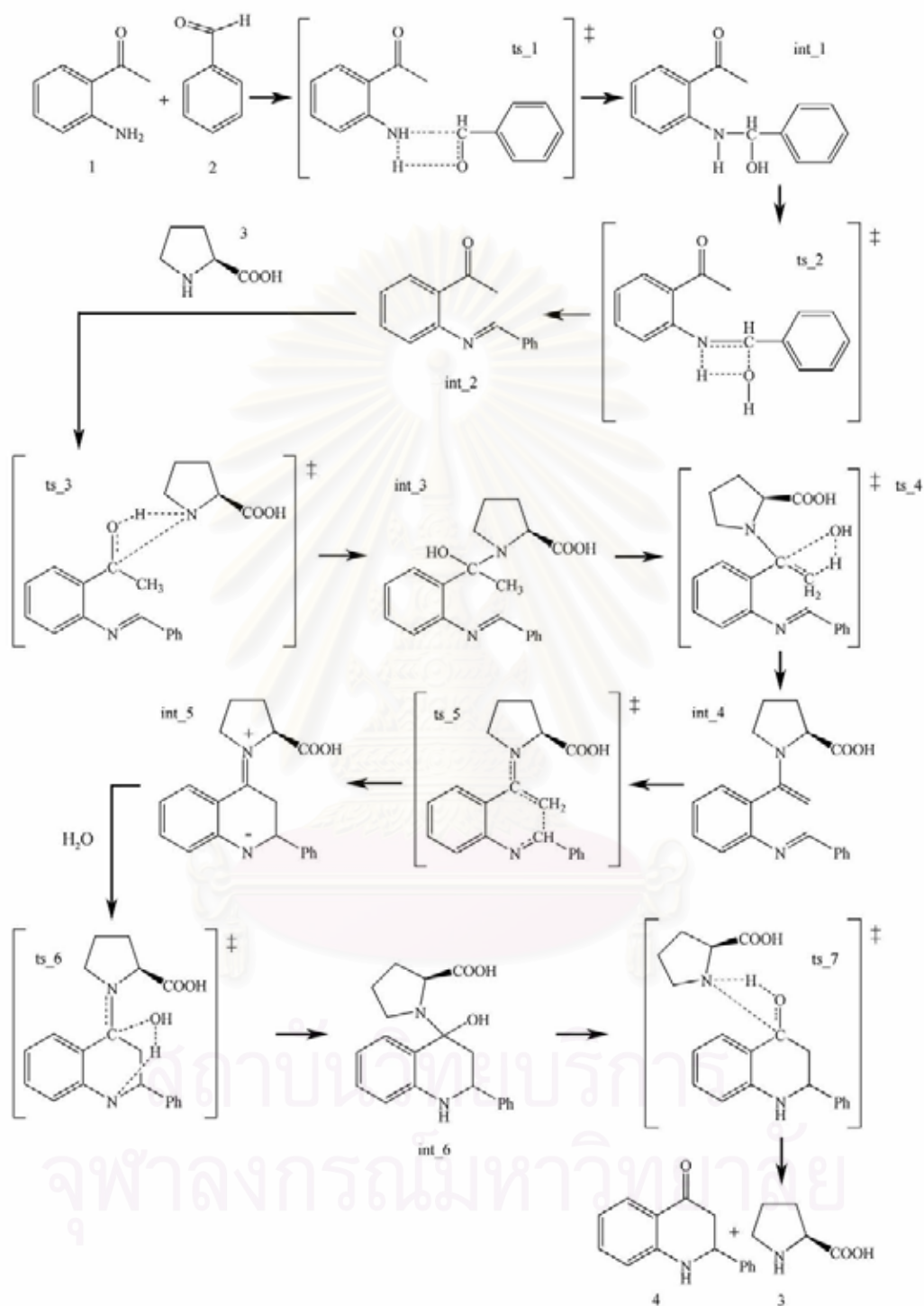


Figure 3.1 An expected reaction mechanisms for the syntheses of the 2-aryl-2,3-dihydroquinolin-4(1H)-one (**P1** or 4)

3.2 Programs used in calculation

All calculations were performed with the GAUSSIAN 03 [14] program. The MOLDEN 4.2 program [20] was utilized to display the molecular structure, monitor the geometrical parameters and observed the molecular geometry convergence *via* the Gaussian output files. The molecular graphics of all related species were generated with the MOLEKEL 4.3 program [21].



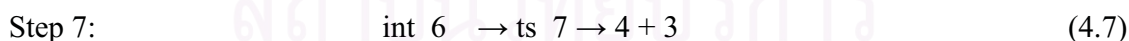
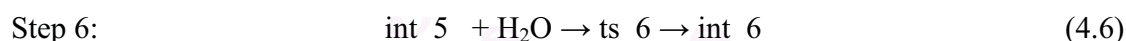
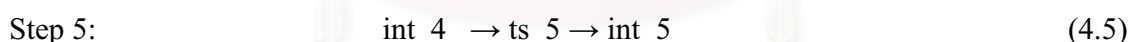
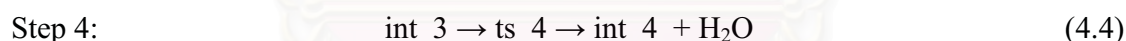
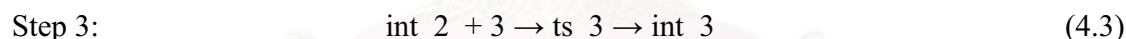
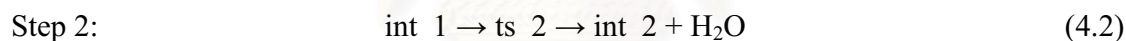
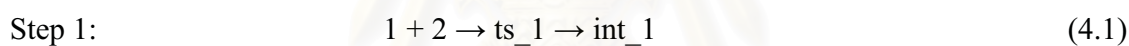
สถาบันวิทยบริการ
จุฬาลงกรณ์มหาวิทยาลัย

CHAPTER IV

RESULTS AND DISCUSSION

Due to the studies of the reaction mechanisms of 4 quinolinone derivatives, all reactions, intermediates, quinolinones products, all involved species and L-proline catalyst were optimized using B3LYP/6-31+G(d,p) and B3LYP/6-31G(d) calculations. Four products as the 2-aryl-2,3-dihydroquinolin-4(1H)-one (**P1**) and its derivatives of which the reactant benzaldehyde are substituted by chloride (*p*-chlorobenzaldehyde) for **P2**, fluoride (*p*-fluorobenzaldehyde) for **P3** and methyl group (*p*-methylbenzaldehyde) for **P4** were studied.

Reaction mechanisms for syntheses of the 2-aryl-2,3-dihydroquinolin-4(1H)-one, **P1** and their derivatives **P2**, **P3** and **P4** are very similar reactions and composed of seven reaction steps. All reaction steps are show as following equation:



The initiation step is the addition reaction between reactants aminoketone (**1**) and aldehyde (**2**) to form intermediate **int_1** via transition state **ts_1**. The second step is dehydration reaction of the **int_1** via transition state **ts_2** to afford **int_2** [11]. The third step is the addition reaction between **int_2** and L-proline catalyst **3** to form **int_3** via transition state **ts_3**. The fourth step is dehydration reaction of the **int_3** via transition

state **ts_4** to form **int_4** [11]. The fifth step is the cyclization reaction of the **int_4** via transition state **ts_5** to form **int_5** [11]. The sixth step is hydration reaction of the **int_5** via transition state **ts_6** to form **int_6**. The last step is the production of the quinolinone **4** via **ts_7**.

4.1 Reaction mechanism for synthesis of **P1**

The reaction mechanism of synthesis of **P1** product and their transition states are shown in Figures 4.1 and 4.2, respectively. Optimized structures shown in both Figures were optimized at the B3LYP/6-31+G(d,p). Energy profile for synthesis reaction of the **P1** product based on the B3LYP/6-31+G(d,p) computation is shown in Figure 4.3 and their structure parameters are shown in Table A1-A17, in Appendix A.

Energies, thermodynamic properties, rate constants and equilibrium constants of synthetic reaction of the 2-aryl-2,3-dihydroquinolin-4(1H)-one (**P1**) catalyzed by L-proline, computed at the B3LYP/6-31+G(d,p) and B3LYP/6-31G(d) levels of theory are shown in Table 4.1. Activation energies, tunneling coefficients, **A** factors and rate constants of synthetic reaction of the **P1** catalyzed by L-proline, computed at the B3LYP/6-31+G(d,p) and B3LYP/6-31G(d) levels are shown in Table 4.2.

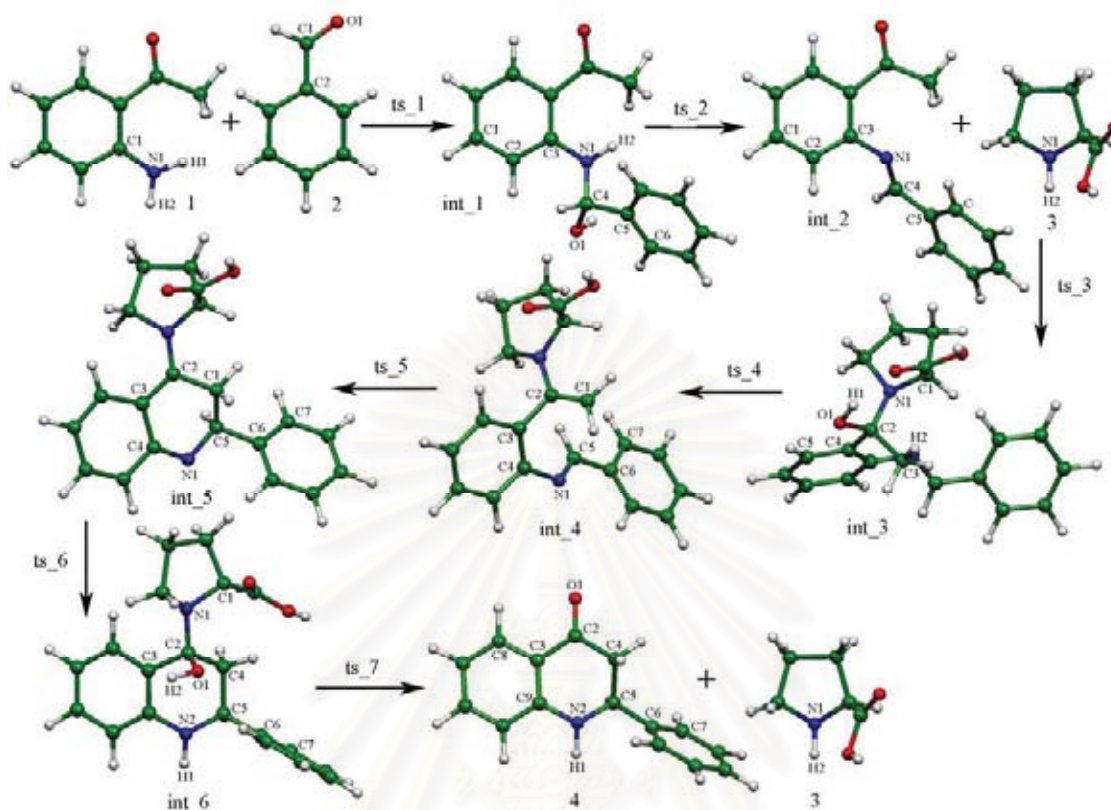


Figure 4.1 Reaction mechanism for synthesis of the 2-aryl-2,3-dihydroquinolin-4(1H)-one, P1.

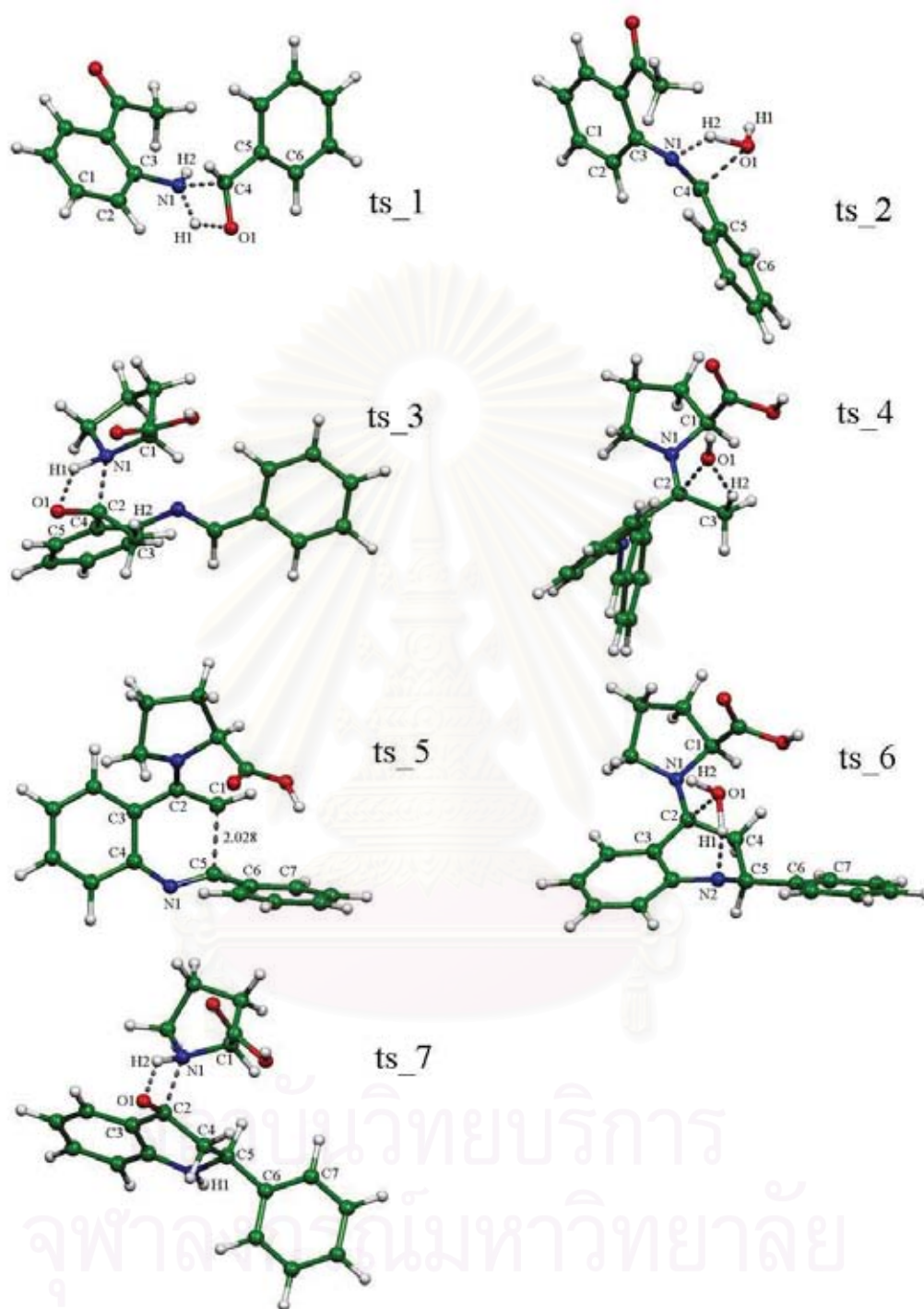


Figure 4.2 The B3LYP/6-31+G(d,p) optimized structures of transition states in reaction mechanism for synthesis of the 2-aryl-2,3-dihydroquinolin-4(1H)-one, **P1**. The imaginary frequency of all transition state are shown in Table A18, Appendix A.

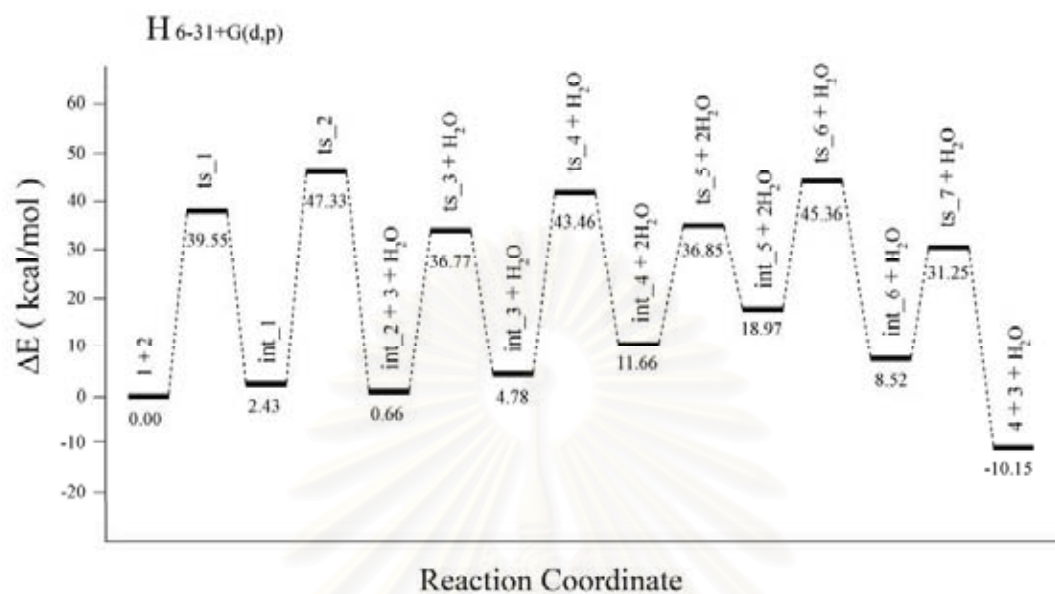


Figure 4.3 Energy profile for synthesis reaction of the 2-aryl-2,3-dihydroquinolin-4(1H)-one.

สถาบันวิทยบริการ
จุฬาลงกรณ์มหาวิทยาลัย

Table 4.1 Energies, thermodynamic properties, rate constants and equilibrium constants of synthetic reaction of the 2-aryl-2,3-dihydroquinolin-4(1H)-one (**P1**) catalyzed by L-proline, computed at the B3LYP/6-31+G(d,p) and B3LYP/6-31G(d) (in parenthesis) levels of theory

Reaction	$\Delta^\ddagger E^{a,b}$	$\Delta^\ddagger G^{a,b}$	k_{298}^c	ΔE^a	ΔG_{298}^a	ΔH_{298}^a	K_{298}
1 + 2 \rightarrow ts_1 \rightarrow int_1	39.55 (39.28)	50.49 (51.43)	6.04×10^{-25} (1.23×10^{-25})	2.43 (1.85)	13.65 (14.59)	3.03 (1.80)	1.01×10^{10} (5.00×10^{10})
int_1 \rightarrow ts_2 \rightarrow int_2 + H ₂ O	44.90 (48.12)	44.79 (47.91)	9.02×10^{-21} (4.65×10^{-23})	-1.77 (4.19)	-11.91 (-6.03)	-0.41 (5.62)	1.87×10^{-9} (3.82×10^{-5})
int_2 + 3 \rightarrow ts_3 \rightarrow int_3	36.11 (36.33)	51.02 (50.97)	2.46×10^{-25} (2.70×10^{-25})	4.13 (2.75)	18.79 (17.18)	3.71 (2.37)	5.98×10^{13} (3.95×10^{12})
int_3 \rightarrow ts_4 \rightarrow int_4 + H ₂ O	38.67 (46.40)	37.98 (46.03)	8.96×10^{-16} (1.12×10^{-21})	6.88 (17.08)	-3.90 (6.19)	8.51 (18.73)	3.43×10^4 (3.43×10^4)
int_4 \rightarrow ts_5 \rightarrow int_5	25.19 (24.06)	26.36 (26.67)	2.93×10^{-7} (1.74×10^{-7})	7.30 (6.67)	8.35 (7.87)	6.67 (6.01)	5.86×10^5 (5.86×10^5)
int_5 + H ₂ O \rightarrow ts_6 \rightarrow int_6	26.39 (20.09)	40.72 (32.34)	8.71×10^{-18} (1.21×10^{-11})	-10.45 (-18.30)	0.62 (-7.20)	-12.05 (-19.90)	2.86×10^0 (5.24×10^{-6})
int_6 \rightarrow ts_7 \rightarrow 4 + 3	22.73 (23.59)	20.51 (22.93)	5.75×10^{-3} (9.68×10^{-5})	-18.67 (-17.29)	-32.78 (-31.47)	-18.56 (-17.18)	9.38×10^{25} (8.45×10^{24})

^a In kcal/mol.

^b Activation energies.

^c In s⁻¹, computed using equation 3.1.

Table 4.1 shows that the B3LYP/6-31+G(d,p) computed free energy of reaction steps 2, 4 and 7 are spontaneous reaction and the rest are non-spontaneous. The reaction steps 2, 6 and 7 are found to be an exothermic reaction.

Table 4.2 Activation energies, tunneling coefficients, A factors and rate constants of synthetic reaction of 2-aryl-2,3-dihydroquinolin-4(1H)-ones (**P1**) catalyzed by L-proline, computed at the B3LYP/6-31+G(d,p) and B3LYP/6-31G(d) (in parenthesis) levels of theory

Reaction	κ^a	Q_{TS}/Q_{REA}	A^b	$\Delta^\ddagger E^{\circ c}$	k_{298}^d
1 + 2 \rightarrow ts_1 \rightarrow int_1	3.88 (4.08)	9.60×10^{-9} (1.25×10^{-9})	5.96×10^4 (7.74×10^3)	39.55 (39.28)	2.35×10^{-24} (5.02×10^{-25})
int_1 \rightarrow ts_2 \rightarrow int_2 + H ₂ O	3.99 (4.39)	1.19×10^0 (1.40×10^0)	7.40×10^{12} (8.71×10^{12})	44.90 (48.12)	3.59×10^{-20} (2.04×10^{-22})
int_2 + 3 \rightarrow ts_3 \rightarrow int_3	3.40 (3.57)	1.18×10^{-11} (1.88×10^{-11})	7.31×10^1 (1.17×10^2)	36.11 (36.33)	8.37×10^{-25} (9.64×10^{-25})
int_3 \rightarrow ts_4 \rightarrow int_4 + H ₂ O	1.14 (1.20)	3.24×10^0 (1.88×10^0)	2.01×10^{13} (1.17×10^{13})	38.67 (46.40)	1.02×10^{-15} (1.34×10^{-21})
int_4 \rightarrow ts_5 \rightarrow int_5	1.19 (1.17)	1.38×10^{-1} (1.21×10^{-2})	8.56×10^{11} (7.54×10^{10})	25.19 (24.06)	3.49×10^{-7} (2.04×10^{-7})
int_5 + H ₂ O \rightarrow ts_6 \rightarrow int_6	2.04 (2.03)	3.06×10^{-11} (1.01×10^{-9})	1.90×10^2 (6.30×10^3)	26.39 (20.09)	1.74×10^{-17} (2.41×10^{-11})
int_6 \rightarrow ts_7 \rightarrow 4 + 3	3.62 (3.73)	4.29×10^1 (3.05×10^0)	2.67×10^{14} (1.90×10^{13})	22.73 (23.59)	2.08×10^{-2} (3.60×10^{-4})

$$^a \kappa = 1 + \frac{1}{24} \left(\frac{h\nu_i}{k_B T} \right)^2.$$

$$^b A = \frac{k_B T}{h} \frac{Q_{TS}}{Q_{REA}}, \text{ in s}^{-1}.$$

^c Computed with ZPVE corrections, in kcal/mol.

^d In s⁻¹, computed using equation 3.2.

Table 4.2 shows the B3LYP/6-31+G(d,p) computed tunneling rate constants of all seven reaction step. We found that rate constants are in decreasing order: step 7 (2.08×10^{-2}) > step 5 (3.49×10^{-7}) > step 4 (1.02×10^{-15}) > step 6 (1.74×10^{-17}) > step 2 (3.59×10^{-20}) > step 1 (2.35×10^{-24}) > step 3 (8.37×10^{-25}). Reaction step 3 is the smallest value of rate constants and they can be considered as rate determining step and also step 1 can be rate determining step due to its value is not different from step 3.

4.2 Reaction mechanism for synthesis of P2

The reaction mechanism of synthesis of **P2** product and their transition states are shown in Figures 4.4 and 4.5, respectively. Optimized structures shown in both Figures were optimized at the B3LYP/6-31+G(d,p). Energy profile for synthesis reaction of the **P2** product based on the B3LYP/6-31+G(d,p) computation is shown in Figure 4.6 and their structure parameters are shown in Table A1-A17, in appendix A.

Energies, thermodynamic properties, rate constants and equilibrium constants of synthetic reaction of the **P2** product catalyzed by L-proline, computed at the B3LYP/6-31+G(d,p) and B3LYP/6-31G(d) levels of theory are shown in Table 4.3. Activation energies, tunneling coefficients, **A** factors and rate constants of synthetic reaction of the **P2** catalyzed by L-proline, computed at the B3LYP/6-31+G(d,p) and B3LYP/6-31G(d) levels are shown in Table 4.4.

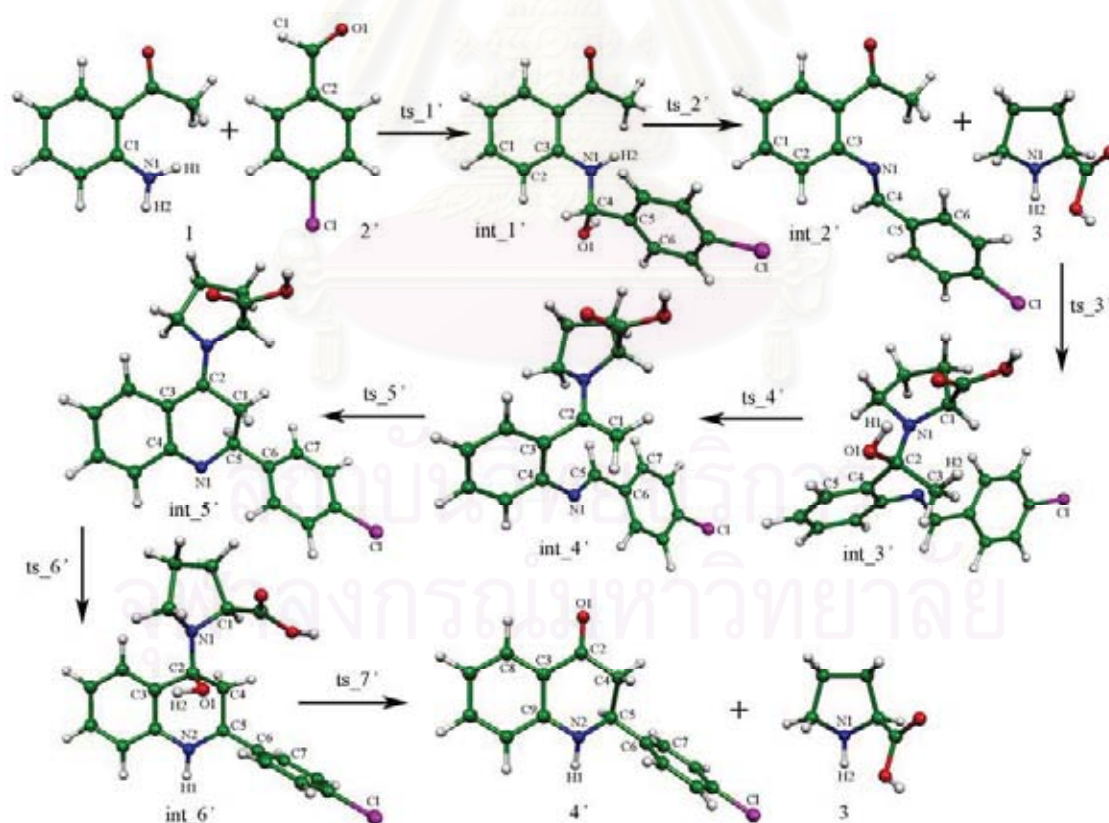


Figure 4.4 Reaction mechanism for synthesis of the **P2** product.

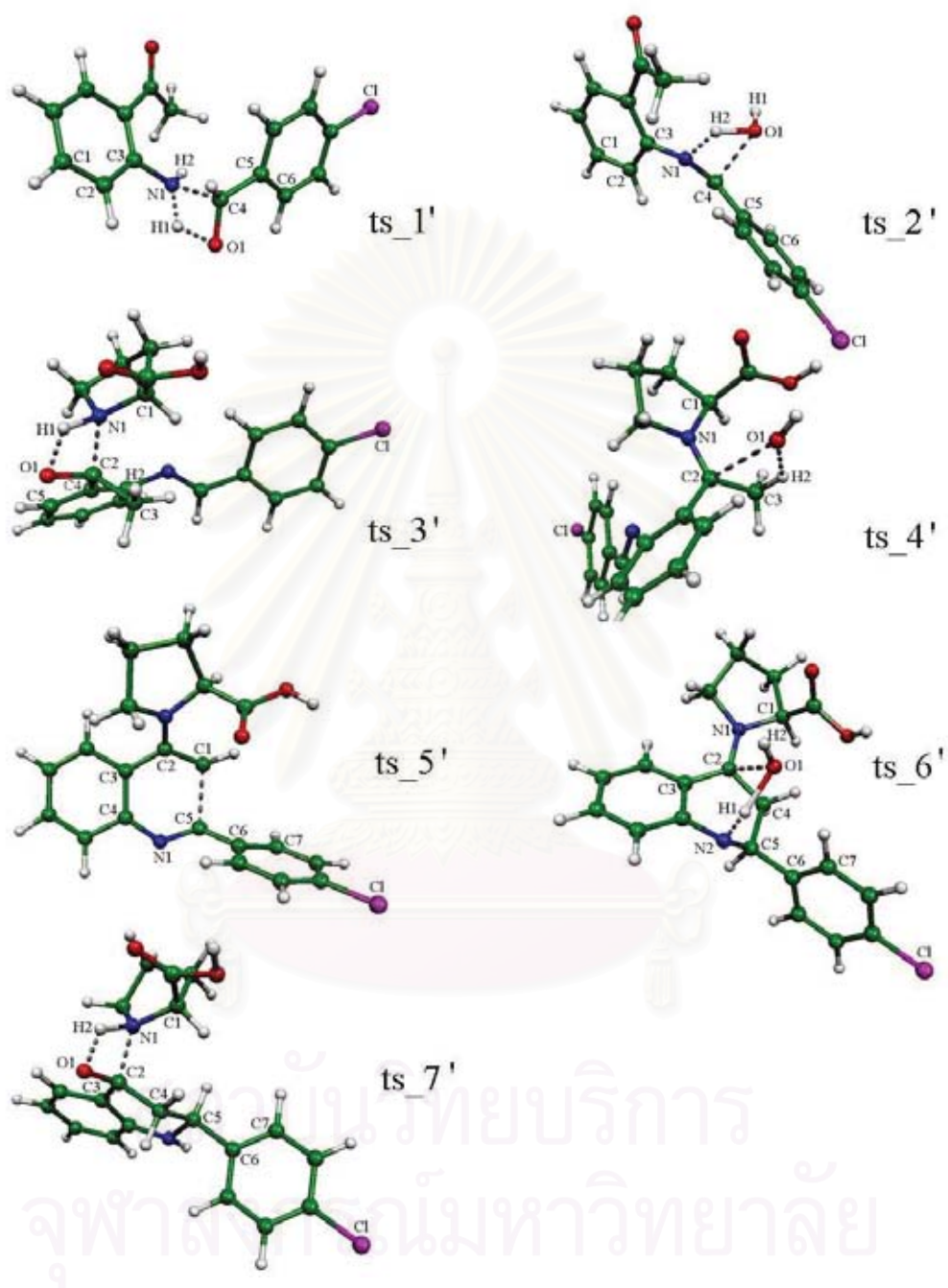


Figure 4.5 The B3LYP/6-31+G(d,p) optimized structures of transition states in reaction mechanism for synthesis of the **P2** product.

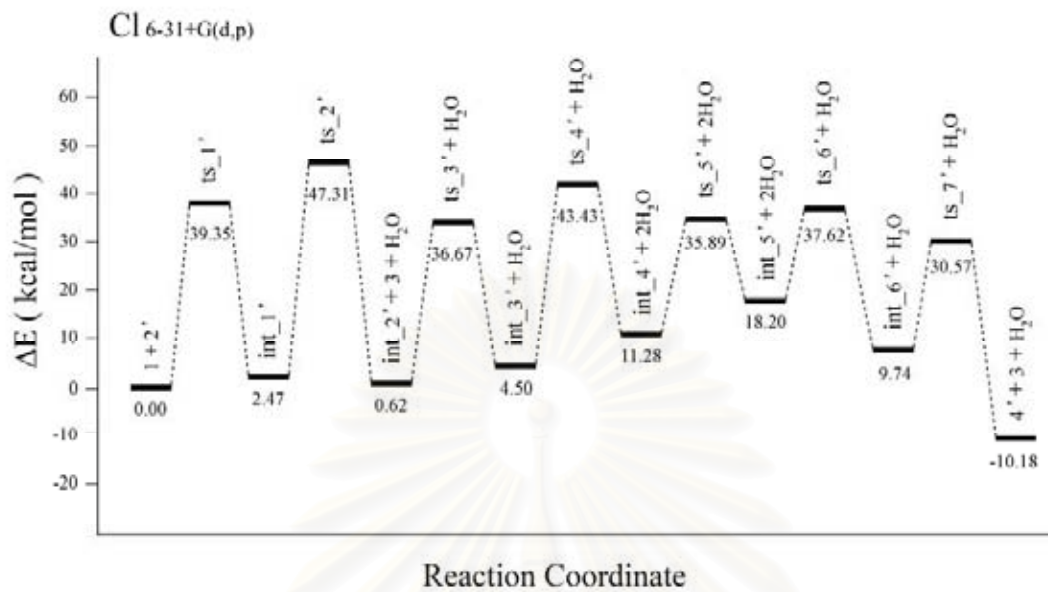


Figure 4.6 Energy profile for synthesis reaction of the **P2** product.

สถาบันวิทยบริการ
จุฬาลงกรณ์มหาวิทยาลัย

Table 4.3 Energies, thermodynamic properties, rate constants and equilibrium constants of synthetic reaction of **P2** product catalyzed by L-proline, computed at the B3LYP/6-31+G(d,p) and B3LYP/6-31G(d) (in parenthesis) levels of theory

Reaction	$\Delta^\ddagger E^{a,b}$	$\Delta^\ddagger G^{a,b}$	k_{298}^c	ΔE^a	ΔG_{298}^a	ΔH_{298}^a	K_{298}
1 + 2' → ts_1' → int_1'	39.35 (39.13)	50.13 (51.47)	1.10 x 10 ⁻²⁴ (1.16 x 10 ⁻²⁵)	2.47 (1.84)	13.56 (14.45)	3.15 (1.87)	8.67 x 10 ⁹ (3.92 x 10 ¹⁰)
int_1' → ts_2' → int_2' + H ₂ O	44.84 (48.09)	44.82 (47.96)	8.64 x 10 ⁻²¹ (4.30 x 10 ⁻²³)	-1.85 (4.12)	-11.87 (-5.93)	-0.53 (5.51)	1.98 x 10 ⁹ (4.50 x 10 ⁻⁵)
int_2' + 3 → ts_3' → int_3'	36.05 (36.22)	50.80 (50.86)	3.60 x 10 ⁻²⁵ (3.24 x 10 ⁻²⁵)	3.88 (2.47)	18.80 (17.08)	3.45 (2.09)	6.10 x 10 ¹³ (3.29 x 10 ¹²)
int_3' → ts_4' → int_4' + H ₂ O	38.93 (46.68)	37.71 (46.22)	1.42 x 10 ⁻¹⁵ (8.08 x 10 ⁻²²)	6.78 (16.96)	-4.41 (5.91)	8.45 (18.63)	5.82 x 10 ⁻⁴ (2.14 x 10 ⁴)
int_4' → ts_5' → int_5'	24.61 (23.94)	26.20 (25.92)	3.88 x 10 ⁻⁷ (6.23 x 10 ⁻⁷)	6.92 (6.13)	7.97 (6.87)	6.26 (5.48)	6.94 x 10 ⁵ (1.08 x 10 ⁵)
int_5' + H ₂ O → ts_6' → int_6'	19.43 (15.36)	31.39 (27.66)	6.07 x 10 ⁻¹¹ (3.30 x 10 ⁻⁸)	-10.26 (-18.00)	1.16 (-6.43)	-11.90 (-19.67)	7.13 x 10 ⁰ (1.95 x 10 ⁻⁵)
int_6' → ts_7' → 4' + 3	22.63 (24.06)	22.01 (23.29)	4.56 x 10 ⁻⁴ (5.28 x 10 ⁻⁵)	-18.12 (-16.70)	-32.43 (-30.81)	-17.97 (-16.55)	1.68 x 10 ⁻²⁴ (2.58 x 10 ⁻²³)

Table 4.3 shows that the B3LYP/6-31+G(d,p) computed free energy of reaction steps 2, 4 and 7 are spontaneous reaction and the rest are non-spontaneous. The reaction steps 2, 6 and 7 are found to be an exothermic reaction.

Table 4.4 Activation energies, tunneling coefficients, A factors and rate constants of synthetic reaction of **P2** product catalyzed by L-proline, computed at the B3LYP/6-31+G(d,p) and B3LYP/6-31G(d) (in parenthesis) levels of theory

Reaction	κ^a	Q_{TS}/Q_{REA}	A^b	$\Delta^\ddagger E^{\circ c}$	k_{298}^d
1 + 2' → ts_1' → int_1'	3.86 (4.02)	1.24×10^{-8} (9.12×10^{-10})	7.72×10^4 (5.66×10^3)	39.35 (39.13)	4.25×10^{-24} (4.68×10^{-25})
int_1' → ts_2' → int_2' + H ₂ O	3.95 (4.42)	1.03×10^0 (1.23×10^0)	6.42×10^{12} (7.67×10^{12})	44.84 (48.09)	3.41×10^{-20} (1.90×10^{-22})
int_2' + 3 → ts_3' → int_3'	3.39 (3.59)	1.57×10^{-11} (1.85×10^{-11})	9.73×10^1 (1.15×10^2)	36.05 (36.22)	1.22×10^{-24} (1.17×10^{-24})
int_3' → ts_4' → int_4' + H ₂ O	1.15 (1.21)	7.83×10^0 (2.15×10^0)	4.86×10^{13} (1.33×10^{13})	38.93 (46.68)	1.62×10^{-15} (9.75×10^{-22})
int_4' → ts_5' → int_5'	1.19 (1.17)	6.82×10^{-2} (3.56×10^{-2})	4.24×10^{11} (2.21×10^{11})	24.61 (23.94)	4.61×10^{-7} (7.32×10^{-7})
int_5' + H ₂ O → ts_6' → int_6'	1.04 (1.99)	1.67×10^{-9} (9.46×10^{-10})	1.04×10^4 (5.88×10^3)	19.43 (15.36)	6.19×10^{-11} (6.43×10^{-8})
int_6' → ts_7' → 4' + 3	3.59 (3.72)	2.87×10^0 (3.72×10^0)	1.78×10^{13} (2.31×10^{13})	22.63 (24.06)	1.63×10^{-3} (1.96×10^{-4})

Table 4.4 shows the B3LYP/6-31+G(d,p) computed tunneling rate constants of all seven reaction step. We found that rate constants are in decreasing order: step 7 (1.63×10^{-3}) > step 5 (4.61×10^{-7}) > step 6 (6.19×10^{-11}) > step 4 (1.62×10^{-15}) > step 2 (3.41×10^{-20}) > step 1 (4.25×10^{-24}) > step 3 (1.22×10^{-24}). Reaction step 3 is the smallest value of rate constants and they can be considered as rate determining step and also step 1 can be rate determining step due to its value is not different from step 3.

4.3 Reaction mechanism for synthesis of P3

The reaction mechanism of synthesis of **P3** product and their transition states are shown in Figures 4.7 and 4.8, respectively. Optimized structures shown in both Figures were optimized at the B3LYP/6-31+G(d,p). Energy profile for synthesis reaction of the **P3** product based on the B3LYP/6-31+G(d,p) computation is shown in Figure 4.9 and their structure parameters are shown in Table A1-A17, in appendix A.

Energies, thermodynamic properties, rate constants and equilibrium constants of synthetic reaction of the **P3** product catalyzed by L-proline, computed at the B3LYP/6-31+G(d,p) and B3LYP/6-31G(d) levels of theory are shown in Table 4.5. Activation energies, tunneling coefficients, **A** factors and rate constants of synthetic reaction of the **P3** catalyzed by L-proline, computed at the B3LYP/6-31+G(d,p) and B3LYP/6-31G(d) levels are shown in Table 4.6.

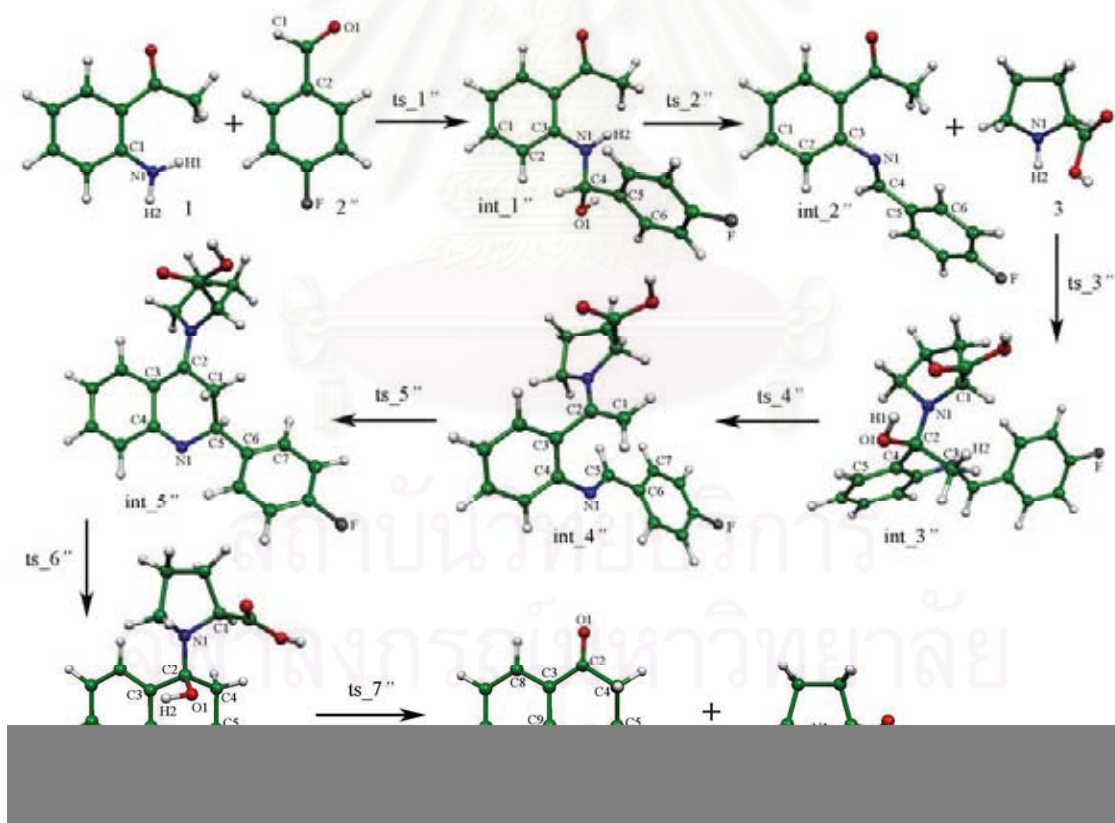


Figure 4.7 Reaction mechanism for synthesis of the **P3** product.

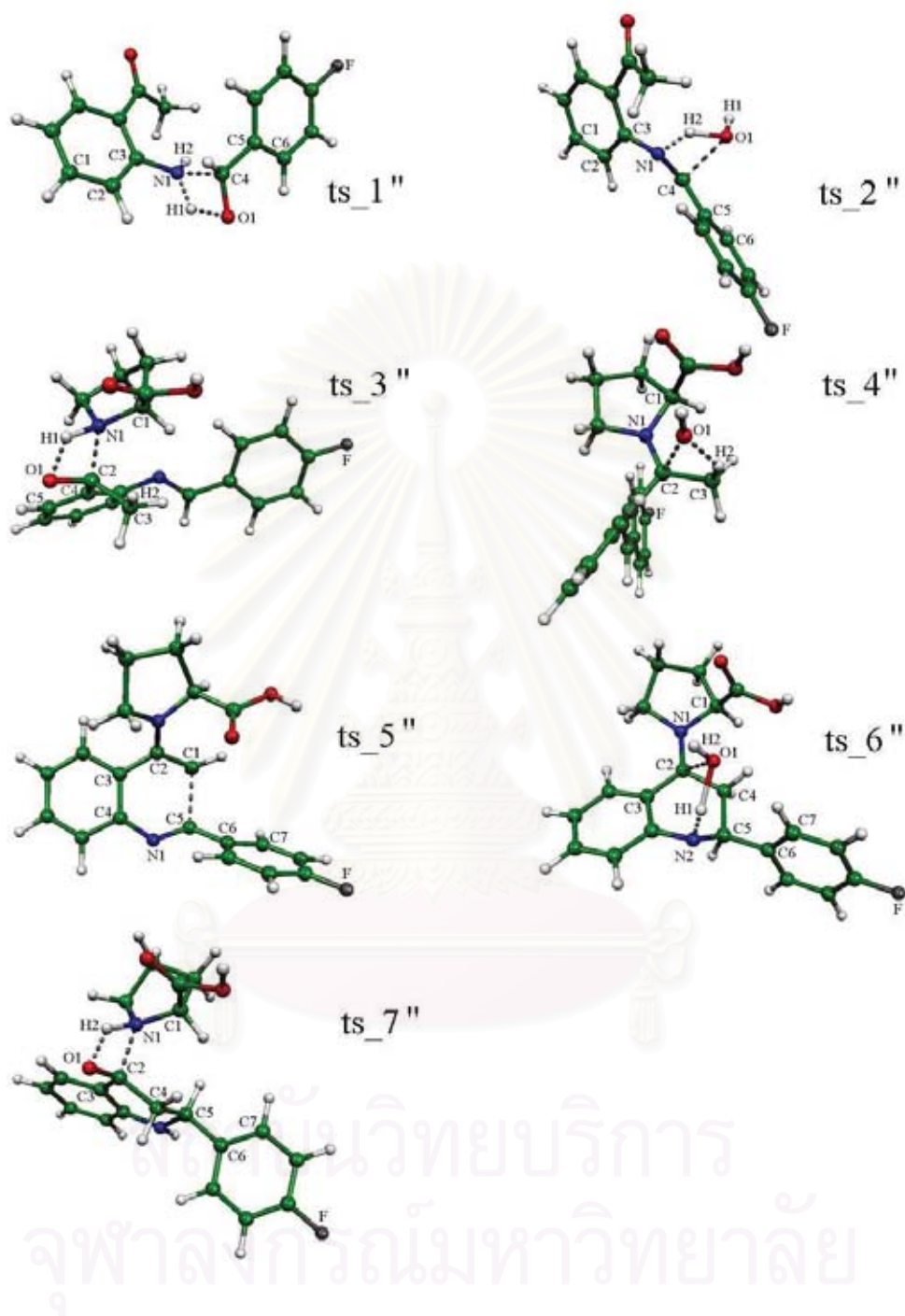


Figure 4.8 The B3LYP/6-31+G(d,p) optimized structures of transition states in reaction mechanism for synthesis of the **P3** product.

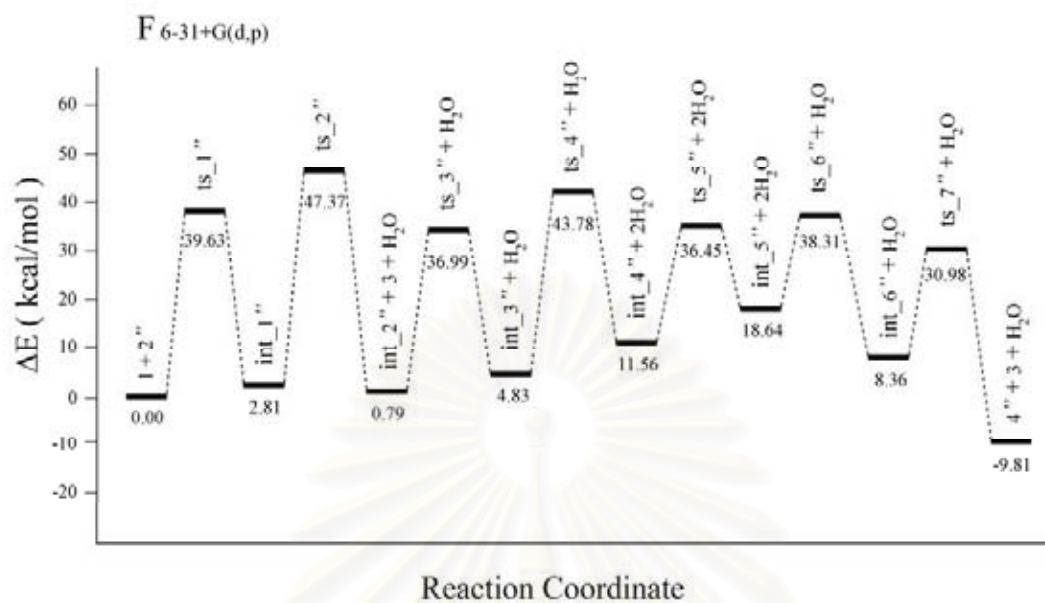


Figure 4.9 Energy profile for synthesis reaction of the **P3** product.

สถาบันวิทยบริการ
จุฬาลงกรณ์มหาวิทยาลัย

Table 4.5 Energies, thermodynamic properties, rate constants and equilibrium constants of synthetic reaction of **P3** product catalyzed by L-proline, computed at the B3LYP/6-31+G(d,p) and B3LYP/6-31G(d) (in parenthesis) levels of theory

Reaction	$\Delta^\ddagger E^{a,b}$	$\Delta^\ddagger G^{a,b}$	k_{298}^c	ΔE^a	ΔG_{298}^a	ΔH_{298}^a	K_{298}
1 + 2'' → ts_1'' → int_1''	39.63 (39.47)	50.51 (51.51)	5.87x10 ⁻²⁵ (1.07 x10 ⁻²⁵)	2.81 (2.34)	13.95 (14.95)	3.47 (2.35)	1.67 x10 ¹⁰ (9.10 x10 ¹⁰)
int_1'' → ts_2'' → int_2'' + H ₂ O	44.56 (47.75)	44.53 (47.64)	1.40 x10 ⁻²⁰ (7.34 x10 ⁻²³)	-2.02 (3.87)	-12.13 (-6.19)	-0.70 (5.26)	1.29 x10 ⁻⁹ (2.91 x10 ⁻⁵)
int_2'' + 3 → ts_3'' → int_3''	36.20 (36.33)	51.16 (51.06)	1.95 x10 ⁻²⁵ (2.30 x10 ⁻²⁵)	4.04 (2.74)	18.98 (17.54)	3.60 (2.31)	8.20 x10 ¹³ (7.18 x10 ¹²)
int_3'' → ts_4'' → int_4'' + H ₂ O	38.95 (46.48)	38.27 (45.88)	5.44 x10 ⁻¹⁶ (1.43 x10 ⁻²¹)	6.73 (16.90)	-4.65 (5.58)	8.42 (18.61)	3.89 x10 ⁻⁴ (1.24 x10 ⁴)
int_4'' → ts_5'' → int_5''	24.89 (24.35)	26.72 (26.33)	1.61 x10 ⁻⁷ (3.12 x10 ⁻⁷)	7.09 (6.63)	8.00 (7.59)	6.47 (6.00)	7.30 x10 ⁵ (3.64 x10 ⁵)
int_5'' + H ₂ O → ts_6'' → int_6''	19.67 (15.38)	32.07 (27.41)	1.93 x10 ⁻¹¹ (4.97 x10 ⁻⁸)	-10.28 (-18.16)	1.50 (-6.54)	-11.97 (-19.84)	1.27 x10 ¹ (1.60 x10 ⁻⁵)
int_6'' → ts_7'' → 4'' + 3	22.61 (23.92)	21.94 (22.98)	5.11 x10 ⁻⁴ (8.90 x10 ⁻⁵)	-18.17 (-16.92)	-32.44 (-31.37)	-18.03 (-16.76)	1.66 x10 ⁻²⁴ (1.02 x10 ⁻²³)

Table 4.5 shows that the B3LYP/6-31+G(d,p) computed free energy of reaction steps 2, 4 and 7 are spontaneous reaction and the rest are non-spontaneous. The reaction steps 2, 6 and 7 are found to be an exothermic reaction.

Table 4.6 Activation energies, tunneling coefficients, A factors and rate constants of synthetic reaction of **P3** product catalyzed by L-proline, computed at the B3LYP/6-31+G(d,p) and B3LYP/6-31G(d) (in parenthesis) levels of theory

Reaction	κ^a	Q_{TS}/Q_{REA}	A^b	$\Delta^\ddagger E^{\circ c}$	k_{298}^d
1 + 2'' → ts_1'' → int_1''	3.86 (4.07)	1.06x10 ⁻⁸ (1.48 x10 ⁻⁹)	6.58 x10 ⁴ (9.20 x10 ³)	39.63 (39.47)	2.27 x10 ⁻²⁴ (4.38 x10 ⁻²⁵)
int_1'' → ts_2'' → int_2'' + H ₂ O	3.90 (4.40)	1.04 x10 ⁰ (1.19 x10 ⁰)	6.49 x10 ¹² (7.41 x10 ¹²)	44.56 (47.75)	5.47 x10 ⁻²⁰ (3.23 x10 ⁻²²)
int_2'' + 3 → ts_3'' → int_3''	3.39 (3.59)	1.08 x10 ⁻¹¹ (1.59 x10 ⁻¹¹)	6.72 x10 ¹ (9.85 x10 ¹)	36.20 (36.33)	6.60 x10 ⁻²⁵ (8.25 x10 ⁻²⁵)
int_3'' → ts_4'' → int_4'' + H ₂ O	1.14 (1.20)	3.12 x10 ⁰ (2.72 x10 ⁰)	1.94 x10 ¹³ (1.69 x10 ¹³)	38.95 (46.48)	6.19 x10 ⁻¹⁶ (1.72 x10 ⁻²¹)
int_4'' → ts_5'' → int_5''	1.19 (1.17)	4.57 x10 ⁻² (3.59 x10 ⁻²)	2.84 x10 ¹¹ (2.23 x10 ¹¹)	24.89 (24.35)	1.91 x10 ⁻⁷ (3.66 x10 ⁻⁷)
int_5'' + H ₂ O → ts_6'' → int_6''	1.03 (1.95)	8.01 x10 ⁻¹⁰ (1.48 x10 ⁻⁹)	4.97 x10 ³ (9.22 x10 ³)	19.67 (15.38)	1.95 x10 ⁻¹¹ (9.51 x10 ⁻⁸)
int_6'' → ts_7'' → 4'' + 3	3.59 (3.72)	3.12 x10 ⁰ (4.95 x10 ⁰)	1.94 x10 ¹³ (3.08 x10 ¹³)	22.61 (23.92)	1.84 x10 ⁻³ (3.31 x10 ⁻⁴)

Table 4.6 shows the B3LYP/6-31+G(d,p) computed tunneling rate constants of all seven reaction step. We found that rate constants are in decreasing order: step 7 (1.84 x10⁻³) > step 5 (1.91 x10⁻⁷) > step 6 (1.95 x10⁻¹¹) > step 4 (6.19 x10⁻¹⁶) > step 2 (5.47 x10⁻²⁰) > step 1 (2.27 x10⁻²⁴) > step 3 (6.60 x10⁻²⁵). Reaction step 3 is the smallest value of rate constants and they can be considered as rate determining step and also step 1 can be rate determining step due to its value is not different from step 3.

4.4 Reaction mechanism for synthesis of P4

The reaction mechanism of synthesis of **P4** product and their transition states are shown in Figures 4.10 and 4.11, respectively. Optimized structures shown in both Figures were optimized at the B3LYP/6-31+G(d,p). Energy profile for synthesis reaction of the **P4** product based on the B3LYP/6-31+G(d,p) computation is shown in Figure 4.12 and their structure parameters are shown in Table A1-A17, in appendix A.

Energies, thermodynamic properties, rate constants and equilibrium constants of synthetic reaction of the **P4** product catalyzed by L-proline, computed at the B3LYP/6-31+G(d,p) and B3LYP/6-31G(d) levels of theory are shown in Table 4.7. Activation energies, tunneling coefficients, **A** factors and rate constants of synthetic reaction of the **P4** catalyzed by L-proline, computed at the B3LYP/6-31+G(d,p) and B3LYP/6-31G(d) levels are shown in Table 4.8.

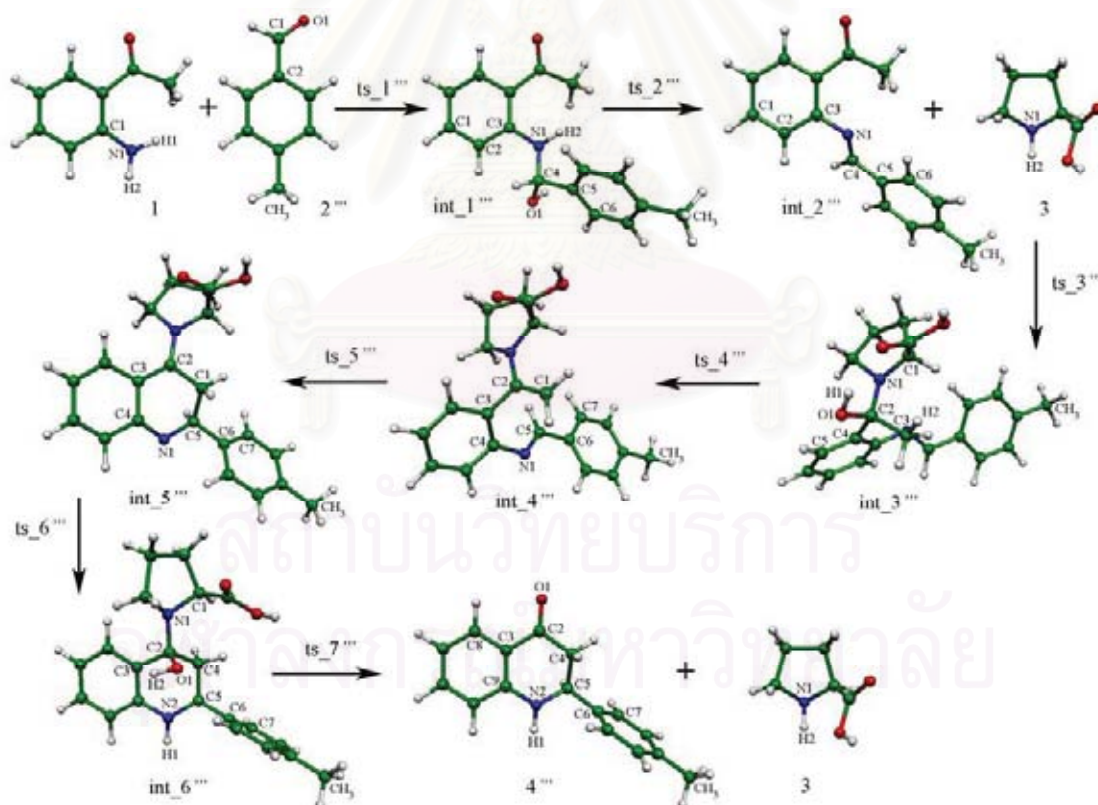


Figure 4.10 Reaction mechanism for synthesis of the **P4** product.

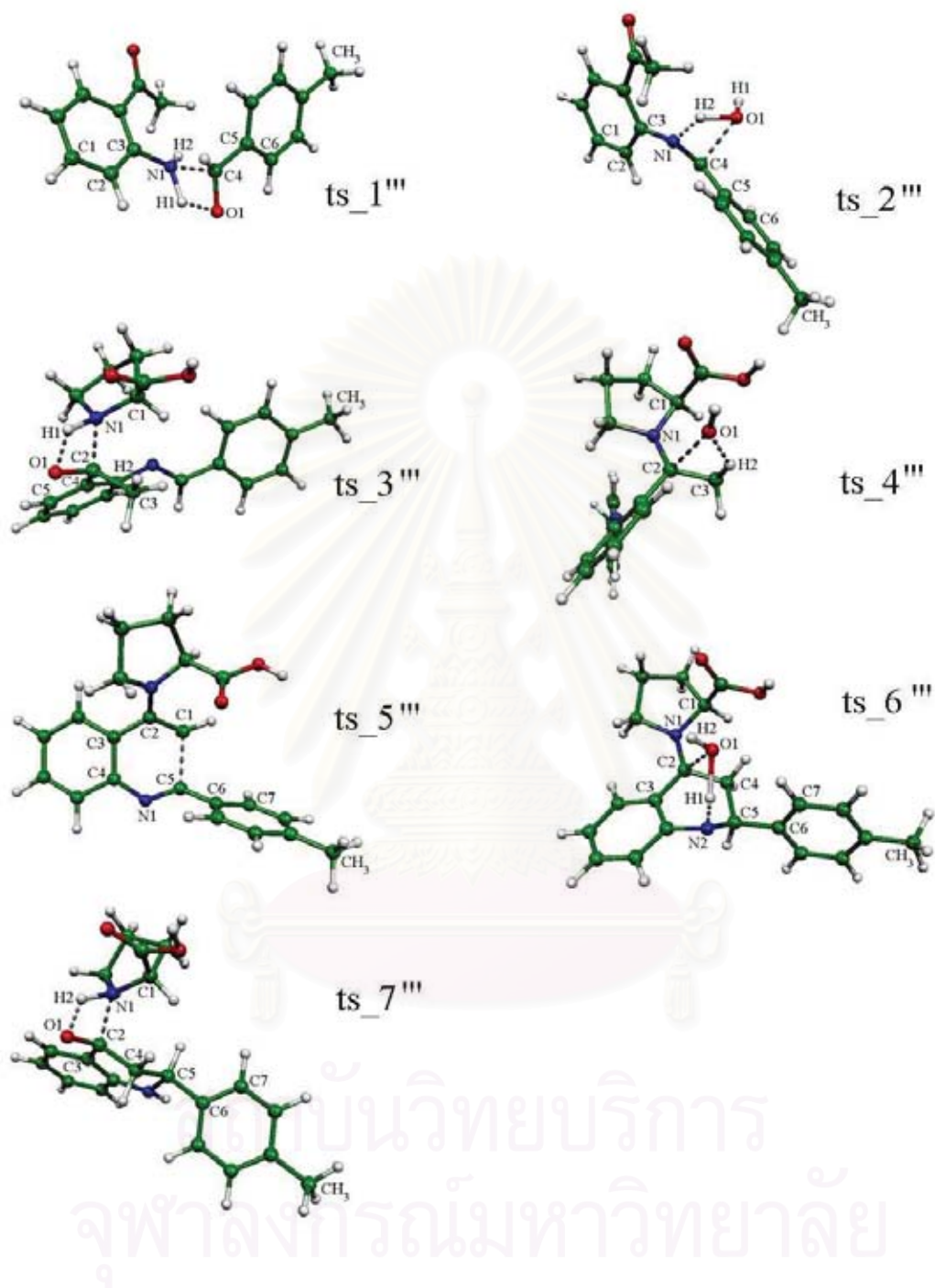


Figure 4.11 The B3LYP/6-31+G(d,p) optimized structures of transition states in reaction mechanism for synthesis of the **P4** product.

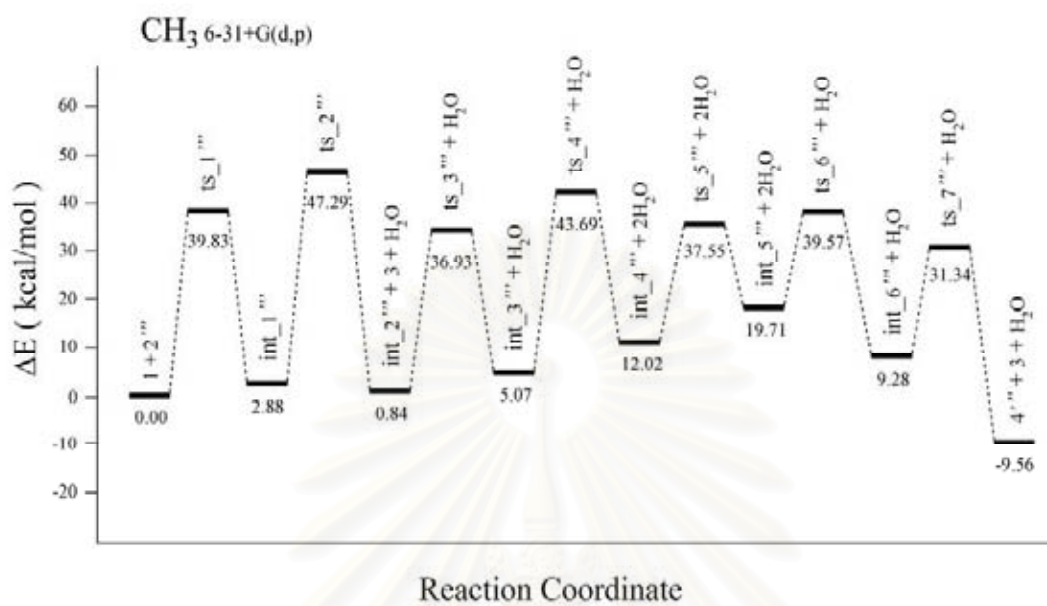


Figure 4.12 Energy profile for synthesis reaction of the **P4** product.

สถาบันวิทยบริการ
จุฬาลงกรณ์มหาวิทยาลัย

Table 4.7 Energies, thermodynamic properties, rate constants and equilibrium constants of synthetic reaction of **P4** product catalyzed by L-proline, computed at the B3LYP/6-31+G(d,p) and B3LYP/6-31G(d) (in parenthesis) levels of theory

Reaction	$\Delta^\ddagger E^{a,b}$	$\Delta^\ddagger G^{a,b}$	k_{298}^c	ΔE^a	ΔG_{298}^a	ΔH_{298}^a	K_{298}
1 + 2''' → ts_1''' → int_1'''	39.83 (39.53)	50.75 (51.90)	3.88x10 ⁻²⁵ (5.62 x10 ⁻²⁶)	2.88 (2.21)	14.25 (15.25)	3.53 (2.19)	2.79 x10 ¹⁰ (1.51 x10 ¹¹)
int_1''' → ts_2''' → int_2''' + H ₂ O	44.41 (47.76)	44.56 (47.72)	1.34 x10 ⁻²⁰ (6.42 x10 ⁻²³)	-2.04 (3.90)	-11.99 (-6.13)	-0.73 (5.30)	1.63 x10 ⁻⁹ (3.21 x10 ⁻⁵)
int_2''' + 3 → ts_3''' → int_3'''	36.09 (36.28)	50.93 (51.03)	2.84 x10 ⁻²⁵ (2.43 x10 ⁻²⁵)	4.23 (2.91)	19.16 (17.42)	3.79 (2.52)	1.12 x10 ¹⁴ (5.88 x10 ¹²)
int_3''' → ts_4''' → int_4''' + H ₂ O	38.62 (46.24)	38.38 (46.71)	4.52 x10 ⁻¹⁶ (3.54 x10 ⁻²²)	6.95 (17.07)	-4.21 (6.22)	8.63 (18.73)	8.25 x10 ⁻⁴ (3.60 x10 ⁴)
int_4''' → ts_5''' → int_5'''	25.53 (24.41)	26.79 (27.31)	1.43 x10 ⁻⁷ (5.94 x10 ⁻⁸)	7.69 (7.02)	8.35 (7.73)	7.11 (6.42)	1.33 x10 ⁶ (4.62 x10 ⁵)
int_5''' + H ₂ O → ts_6''' → int_6'''	19.86 (15.66)	32.11 (27.69)	1.80 x10 ⁻¹¹ (3.10 x10 ⁻⁸)	-10.43 (-18.27)	1.33 (-6.70)	-12.13 (-19.94)	9.51 x10 ⁰ (1.22 x10 ⁻⁵)
int_6''' → ts_7''' → 4''' + 3	22.06 (23.53)	21.34 (22.78)	1.40 x10 ⁻³ (1.25 x10 ⁻⁴)	-18.84 (-17.44)	-33.09 (-31.75)	-18.71 (-17.31)	5.56 x10 ⁻²⁵ (5.26 x10 ⁻²⁴)

Table 4.7 shows that the B3LYP/6-31+G(d,p) computed free energy of reaction steps 2, 4 and 7 are spontaneous reaction and the rest are non-spontaneous. The reaction steps 2, 6 and 7 are found to be an exothermic reaction.

Table 4.8 Activation energies, tunneling coefficients, A factors and rate constants of synthetic reaction of **P4** product catalyzed by L-proline, computed at the B3LYP/6-31+G(d,p) and B3LYP/6-31G(d) (in parenthesis) levels of theory

Reaction	κ^a	Q_{TS}/Q_{REA}	A^b	$\Delta^\ddagger E^{\circ c}$	k_{298}^d
1 + 2''' → ts_1''' → int_1'''	3.94 (4.15)	9.89×10^{-9} (8.66×10^{-10})	6.14×10^4 (5.38×10^3)	39.83 (39.53)	1.53×10^{-24} (2.34×10^{-25})
int_1''' → ts_2''' → int_2''' + H ₂ O	3.76 (4.38)	7.73×10^{-1} (1.07×10^0)	4.80×10^{12} (6.64×10^{12})	44.41 (47.76)	5.02×10^{-20} (2.81×10^{-22})
int_2''' + 3 → ts_3''' → int_3'''	3.38 (3.59)	1.32×10^{-11} (1.56×10^{-11})	8.22×10^1 (9.66×10^1)	36.09 (36.28)	9.64×10^{-25} (8.72×10^{-25})
int_3''' → ts_4''' → int_4''' + H ₂ O	1.13 (1.19)	1.49×10^0 (4.51×10^{-1})	9.28×10^{12} (2.80×10^{12})	38.62 (46.24)	5.09×10^{-16} (4.21×10^{-22})
int_4''' → ts_5''' → int_5'''	1.19 (1.17)	1.19×10^{-1} (7.55×10^{-3})	7.39×10^{11} (4.69×10^{10})	25.53 (24.41)	1.70×10^{-7} (6.98×10^{-8})
int_5''' + H ₂ O → ts_6''' → int_6'''	1.04 (2.02)	1.03×10^{-9} (1.48×10^{-9})	6.41×10^3 (9.17×10^3)	19.86 (15.66)	1.83×10^{-11} (6.13×10^{-8})
int_6''' → ts_7''' → 4''' + 3	3.60 (3.73)	3.36×10^0 (3.54×10^0)	2.08×10^{13} (2.20×10^{13})	22.06 (23.53)	5.05×10^{-3} (4.64×10^{-4})

Table 4.8 shows the B3LYP/6-31+G(d,p) computed tunneling rate constants of all seven reaction step. We found that rate constants are in decreasing order: step 7 (5.05×10^{-3}) > step 5 (1.70×10^{-7}) > step 6 (1.83×10^{-11}) > step 4 (5.09×10^{-16}) > step 2 (5.02×10^{-20}) > step 1 (1.53×10^{-24}) > step 3 (9.64×10^{-25}). Reaction step 3 is the smallest value of rate constants and they can be considered as rate determining step and also step 1 can be rate determining step due to its value is not different from step 3.

In this work we study in 4 difference substituent. For synthesis 4 quinolinone derivatives, substituent on para-position (H) of reactant benzaldehyde was replaced with Cl, F and CH₃.

The rate constant of step 3 of all systems (**P1**, **P2**, **P3** and **P4**) is found to be the smallest value. It can be considered as rate determining step. Based on the smallest rate constant (step 3) their magnitude is in decreasing order: **P2** (1.22×10^{-24}) > **P4** (9.64×10^{-25}) > **P1** (8.37×10^{-25}) > **P3** (6.60×10^{-25}).

In Figure 4.13 showed that int_3 was synthesized by nucleophilic substitution of catalyst L-proline and int_2, which R = H, Cl, F and CH₃. The results from computational calculation exhibited the reactivity of substitution are Cl, CH₃, H and F, respectively. We have questioned that the substitution of amine L-proline to the various carbonyl carbon is non-significance because R-substituent of int_2 is located to far from reaction site.

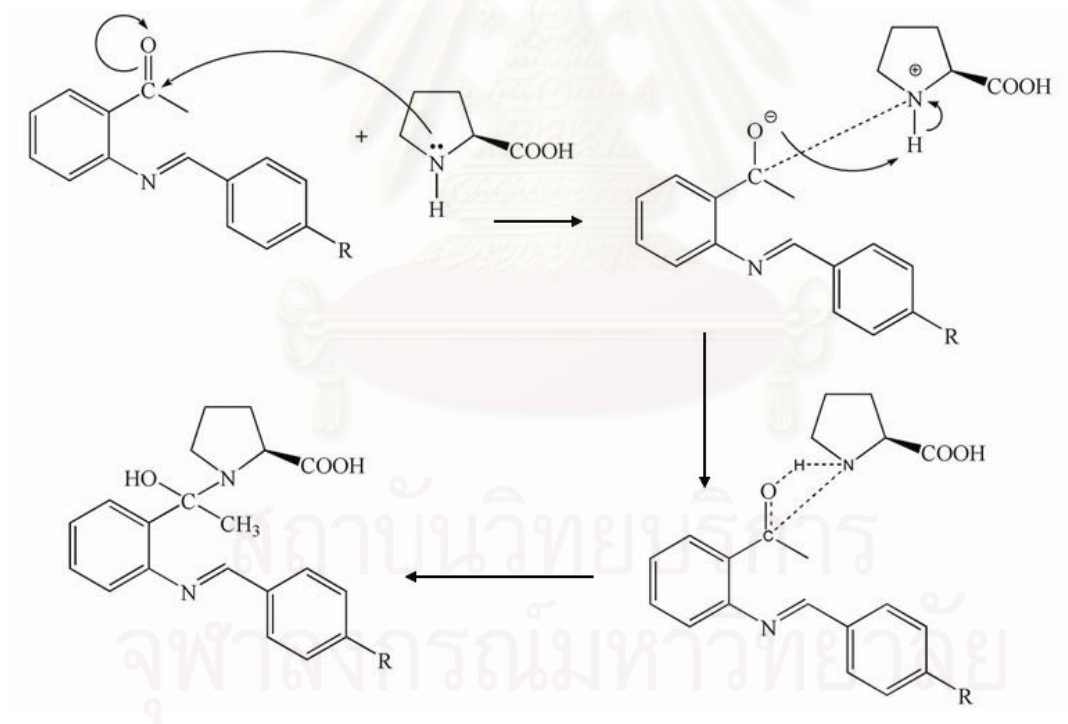


Figure 4.13 Mechanism of step 3, nucleophilic substitution of catalyst L-proline and int_2 to form int_3.

All reaction quantities namely activation energy, free energy of activation, energy, enthalpy and free energy of reactions computed at B3LYP/6-31+G(d,p) are mostly less than those obtained by the B3LYP/6-31G(d). These values correspond to results of many works [22, 23]. Nevertheless, the B3LYP/6-31+G(d,p) should give more good results because our studied compounds contain atom such as N and O atoms.

In this work we computed rate constant of reactions using two different formulas which based on the transition-state theory, These two formulas are based on the Gibbs free energy of activation ($\Delta^\ddagger G^0$) and activation energy ($\Delta^\ddagger E$) as

$$k(T) = \frac{k_B T}{hc^0} \exp(-\Delta^\ddagger G^0 / RT) \quad \text{and} \quad k = \kappa \left[\frac{k_B T}{h} \right] \left[\frac{Q_{TS}}{Q_{REA}} \right] \exp(-\Delta^\ddagger E / RT),$$

respectively.

The pre-exponential factor for the second formula depend upon the tunneling coefficient and partition functions ratios and this should give more reliable that the first formula because c^0 of first one is approximate to unity.

CHAPTER V

CONCLUSION

In this study, we can conclude as the following remarks:

- All reactions of studied systems (**P1**, **P2**, **P3** and **P4**) are composed of the same mechanism:

Step 1 is the addition reaction between reactants *o*-aminoacetophenone (**1**) and benzaldehyde (**2**) to form intermediate **int_1** via transition state **ts_1**.

Step 2 is dehydration reaction of the **int_1** via transition state **ts_2** to afford **int_2**.

Step 3 is the addition reaction between **int_2** and L-proline catalyst **3** to form **int_3** via transition state **ts_3**.

Step 4 is dehydration reaction of the **int_3** via transition state **ts_4** to form **int_4**.

Step 5 is the intramolecular cyclization of the **int_4** via transition state **ts_5** to form **int_5**.

Step 6 is hydration reaction of the **int_5** via transition state **ts_6** to form **int_6**.

Step 7 is the production of the quinolinone **4** via **ts_7**.

- The order of rate constants of reactions for all systems (**P1**, **P2**, **P3** and **P4**) are in decreasing order:

System **P1** : step 7 > step 5 > step 4 > step 6 > step 2 > step 1 > step 3.

System **P2** : step 7 > step 5 > step 6 > step 4 > step 2 > step 1 > step 3.

System **P3** : step 7 > step 5 > step 6 > step 4 > step 2 > step 1 > step 3.

System **P4** : step 7 > step 5 > step 6 > step 4 > step 2 > step 1 > step 3.

The rate constant of step 3 of all systems is found to be the smallest value. We can conclude that rate determining step of synthetic reactions for products P1, P2, P3 and P4 are step 3.

- Based on the smallest rate constant (step 3), their values are in decreasing order: **P2** (1.22×10^{-24}) > **P4** (9.64×10^{-25}) > **P1** (8.37×10^{-25}) > **P3** (6.60×10^{-25}). Due to this order, there are non-significant effects of substituents to the synthetic reaction of quinolinone.

Suggestion for future work

Mechanisms for synthetic reaction of these quinolinone derivatives using other amine compounds as catalysts are suggested to be investigated using the same theory of calculations in order to compare these catalytic properties to the results of this work. These suggested amino-compound catalysts should be also compared with the L-proline catalyst in terms of their stereo-selectivity.



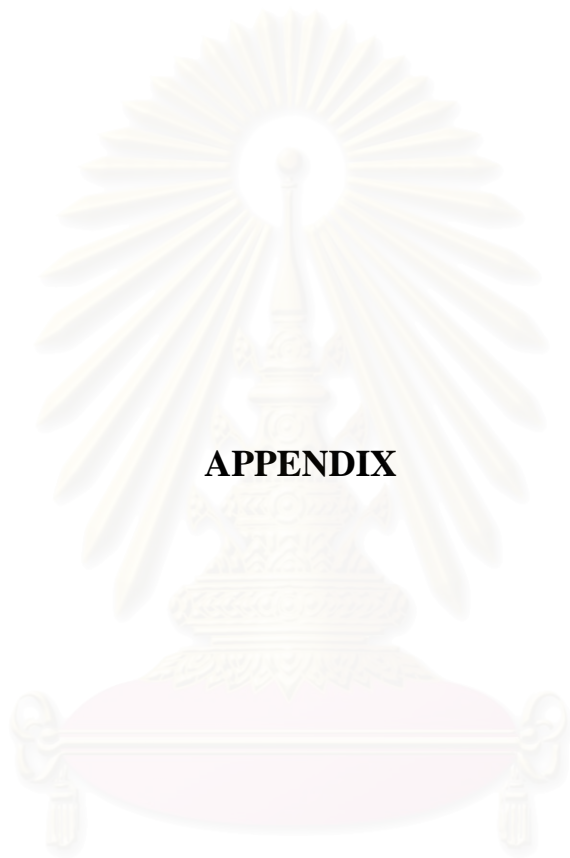
สถาบันวิทยบริการ
จุฬาลงกรณ์มหาวิทยาลัย

REFERENCES

- [1] Ragaini, F.; Sportiello, P.; Cenini, S. Investigation of the possible role of arylamine formation in the *ortho*-substituted nitroarenes reductive cyclization reactions to afford heterocycles, *J. Organomet. Chem.* 577 (1999): 283–291.
- [2] Lee, A. S.; Tsao, K.; Chang, Y.; Chu, S. L-Proline-catalyzed intramolecular cyclization of 5-hydroxypentene to β -halogenated tetrahydrofuran, *Tetrahedron Lett.* 48 (2007): 6790–6793.
- [3] Pak, C. S.; Choi, E. B.; Yon, G. H.; Yang, H. C.; Lee, H. K.; Lee, G. H.; Lee, J. P.; Choi, G. J. 4-Amino-2-quinolinone derivatives, US Patent 5707931. (1998).
- [4] Parish, L. C.; Witkowski, J. A.; Routh, H. B. Moxifloxacin for the treatment of Bacterial Skin Infections, skin therapy letter. 6 (2001): 1-2.
- [5] Sit, S. Y.; Meanwell, N. A. 4-Aryl-3-hydroxyquinolin-2-one derivatives as ion channel modulators, WO Patent 023273. (1998).
- [6] Arcadi, A.; Marinelli, F.; Rossii, E. Synthesis of functionalised quinolines through tandem addition /annulation reactions of β -(2-aminophenyl)- α , β – ynones, *Tetrahedron.* 55 (1999): 13233-13250.
- [7] Wang, M. X.; Liu, Y.; Huang, Z. T. Novel and convenient synthesis of polyfunctionalized quinolines,quinolones and their annulation reactions *Tetrahedron Lett.* 42 (2001): 2553–2555.
- [8] Bahmanyar, S.; Houk, K. N.; Martin, H. J.; List, B. Quantum mechanical predictions of the stereoselectivities of proline-catalyzed asymmetric intermolecular aldol reactions, *J. Am. Chem. Soc.* 125 (2003): 2475
- [9] Park, M. S.; Lee, J. I. Synthesis of new 2,3-dihydro-2-phenyl-4-quinolone derivatives; aza analogs of flavanone, *Bull. Korean Chem. Soc.* 25 (2004): 1269-1272.
- [10] Sabitha, G.; Kumar, M. R.; Reddy, M. S. K.; Yadav, J. S.; Krishna, K. V. S. R.; Kunwar, A. C. A D,L-proline catalyzed diastereoselective trimolecular condensation: an approach to the one-pot synthesis of perhydrofuro[3,2-b]pyran-5-ones, *Tetrahedron Lett.* 46 (2005): 1659–1661.

- [11] Chandrasekhar, S.; Vijeender, K.; Sridhar, C. L-Proline-catalyzed one-pot synthesis of 2-aryl-2,3-dihydroquinolin-4(1H)-ones, *Tetrahedron Lett.* 48 (2007): 4935–4937.
- [12] Jensen, F. *Introduction to computational chemistry*. Chichester: John Wiley & Sons, (1999).
- [13] Lewars, E. *Computational chemistry: Introduction to the theory and applications of molecular and quantum mechanics*. Trent University: Peterborough, Ontario, (2003).
- [14] Frisch, M. J.; Trucks, G. W.; Schlegel, H. B.; Scuseria, G. E.; Robb, M. A.; Cheeseman, J. R.; Montgomery, J. A.; Jr.; Vreven, T.; Kudin, K. N.; Burant, J. C.; Millam, J. M.; Iyengar, S. S.; Tomasi, J.; Barone, V.; Mennucci, B.; Cossi, M.; Scalmani, G.; Rega, N.; Petersson, G. A.; Nakatsuji, H.; Hada, M.; Ehara, M.; Toyota, K.; Fukuda, R.; Hasegawa, J.; Ishida, M.; Nakajima, T.; Honda, Y.; Kitao, O.; Nakai, H.; Klene, M.; Li, X.; Knox, J. E.; Hratchian, H. P.; Cross, J. B.; Adamo, C.; Jaramillo, J.; Gomperts, R.; Stratmann, R. E.; Yazyev, O.; Austin, A. J.; Cammi, R.; Pomelli, C.; Ochterski, J. W.; Ayala, P. Y.; Morokuma, K.; Voth, G. A.; Salvador, P.; Dannenberg, J. J.; Zakrzewski, V. G.; Dapprich, S.; Daniels, A. D.; Strain, M. C.; Farkas, O.; Malick, D. K.; Rabuck, A. D.; Raghavachari, K.; Foresman, J. B.; Ortiz, J. V.; Cui, Q.; Baboul, A. G.; Clifford, S.; Cioslowski, J.; Stefanov, B. B.; Liu, G.; Liashenko, A.; Piskorz, P.; Komaromi, I.; Martin, R. L.; Fox, D. J.; Keith, T.; Al-Laham, M. A.; Peng, C. Y.; Nanayakkara, A.; Challacombe, M.; Gill, P. M. W.; Johnson, B.; Chen, W.; Wong, M. W.; Gonzalez, C. and Pople, J. A. *Gaussian 03. Revision B.03*: Gaussian, Inc., Pittsburgh PA, (2003).
- [15] Anton, V. J.; Stanislav, Z. Modeling of charge-transfer transitions and excited states in d6 transition metal complexes by DFT techniques coordination. *Chem. Rev.* 251 (2007): 258–287.
- [16] Domingo, R. L.; Saez, A. J.; Palmucci, C.; Arquesb, S. J.; Gonzalez-Rosendec, E. M. A DFT study for the formation of imidazo [1,2-c] pyrimidines through an intramolecular Michael addition. *Tetrahedron.* 62 (2006): 10408–10416.
- [17] Becke, D. A. Density-Functional Thermochemistry .3. the Role of Exact exchange. *J. Chem. Phys.* 98 (1993): 5648.

- [18] Becke, D. Density-functional exchange-energy approximation with correct asymptotic behavior. *Phys. Rev. A.* 38 (1988): 3098.
- [19] Lee, C.; Yang, W.; Parr, R.G. Development of the Colle-Salvetti correlation energy formula into a functional of the electron density. *Phys. Rev. B.* 37 (1988): 785.
- [20] Schaftenaar, G. MOLDEN 4.2 CAOS/CAMM, Center Nijmegen Toernooiveld, Nijmegen (Netherlands), 1991.
- [21] Flükiger, P.; Lüthi, P. H.; Portmann, S.; Weber, J. MOLEKEL 4.3, Swiss Center for Scientific Computing, Manno (Switzerland), 2000.
- [22] Julian, T.; William L. J. Performance of B3LYP Density Functional Methods for a large set of organic molecules, *J. Chem. Theory Comput.* 4 (2008): 297-306.
- [23] Csonka, G. I. Proper basis set for Quantum mechanical studies of potential energy surfaces of carbohydrates, *J. Mol. Struct.* 584 (2000): 1-4.



APPENDIX

สถาบันวิทยบริการ
จุฬาลงกรณ์มหาวิทยาลัย

APPENDIX A

Table A1 Selected geometry parameters for ts_1, ts_1', ts_1'' and ts_1'''.

Dihedral angle	Compounds			
	ts_1	ts_1'	ts_1''	ts_1'''
C1-C2-C3-N1	175.9	175.8	175.7	175.8
C3-N1-C4-C5	-115.1	-115.0	-115.2	-114.3
O1-C4-C5-C6	13.9	12.3	12.3	13.5
Bond length (Å)				
N1-C4	1.712	1.702	1.708	1.731
H1-O1	1.327	1.332	1.328	1.317
N1-H1	1.231	1.230	1.231	1.237
C4-O1	1.339	1.340	1.340	1.338

Table A2 Selected geometry parameters for ts_2, ts_2', ts_2'' and ts_2'''.

Dihedral angle	Compounds			
	ts_1	ts_1'	ts_1''	ts_1'''
C1-C2-C3-N1	-178.2	-178.2	-178.2	-178.2
C3-N1-C4-C5	-149.0	-149.7	-149.6	-149.6
O1-C4-C5-C6	-93.0	-92.9	-92.8	-93.9
Bond length (Å)				
N1-C2	1.641	1.642	1.644	1.643
H1-O1	1.348	1.347	1.347	1.347
C2-O1	1.363	1.362	1.362	1.362
H1-N1	1.219	1.219	1.219	1.219
N1-C2	1.641	1.642	1.644	1.643

Table A3 Selected geometry parameters for ts_3, ts_3', ts_3'' and ts_3'''.

Dihedral angel	Compounds			
	ts_3	ts_3'	ts_3''	ts_3'''
C1-N1-C2-C3	15.5	15.7	14.4	14.6
N1-H1-O1-C2	14.4	14.4	13.8	13.8
O1-C2-C4-C5	-7.8	-7.2	-7.6	-7.7
Bond length (Å°)				
N1-C2	1.641	1.642	1.644	1.643
H1-O1	1.348	1.347	1.347	1.347
C2-O1	1.363	1.362	1.362	1.362
H1-N1	1.219	1.219	1.219	1.219

Table A4 Selected geometry parameters for ts_4, ts_4', ts_4'' and ts_4'''.

Dihedral angel	Compounds			
	ts_4	ts_4'	ts_4''	ts_4'''
C1-N1-C2-C3	-4.9	-5.4	-5.3	-5.2
O1-C2-C3-H2	4.6	4.3	4.5	4.7
Bond length (Å°)				
N1-C2	1.319	1.319	1.319	1.319
C2-O1	2.515	2.509	2.513	2.523
C3-H2	1.167	1.167	1.330	1.164
O1-H2	1.583	1.581	1.582	1.588
C2-C3	1.463	1.463	1.463	1.464

สถาบันวิทยบริการ
จุฬาลงกรณ์มหาวิทยาลัย

Table A5 Selected geometry parameters for ts_5, ts_5', ts_5'' and ts_5'''.

Dihedral angel	Compounds			
	ts_5	ts_5'	ts_5''	ts_5'''
C1-C2-C3-C4	46.8	47	46.8	46.5
C3-C4-N1-C5	-38.5	-38.7	-38.4	-37.9
N1-C5-C6-C7	155.3	155.5	155.2	155.0
Bond length (Å°)				
C1-C5	2.023	2.024	2.023	2.023
C1-C2	1.423	1.423	1.423	1.423
C4-N1	1.340	1.342	1.341	1.340
N1-C5	1.350	1.350	1.350	1.351
C5-C6	1.494	1.494	1.494	1.493

Table A6 Selected geometry parameters for ts_6, ts_6', ts_6'' and ts_6'''.

Dihedral angel	Compounds			
	ts_6	ts_6'	ts_6''	ts_6'''
C1-N1-C2-C3	175.6	174.9	174.8	174.1
H1-O1-C2-C3	49.6	43.9	44.1	44.8
C4-C5-C6-C7	-47.6	-108.4	-108.4	-107.8
Bond length (Å°)				
C2-O1	2.198	2.672	2.676	2.678
O1-H1	1.149	1.482	1.492	1.489
H1-N2	1.420	1.125	1.121	1.123
H2-O1	0.996	0.967	0.967	0.967

สถาบันวิทยบริการ
จุฬาลงกรณ์มหาวิทยาลัย

Table A7 Selected geometry parameters for ts_7, ts_7', ts_7'' and ts_7'''.

Dihedral angel				
	ts_7	ts_7'	ts_7''	ts_7'''
C1-N1-C2-C3	-140.9	-134.4	-134.4	-134.6
H2-O1-C2-C3	-106.7	-111.5	-111.5	-111.3
C4-C5-C6-C7	-102.6	-104.0	-105.4	-105.1
Bond length (Å°)				
N1-C2	1.732	1.729	1.73	1.734
H2-O1	1.307	1.303	1.303	1.301
H2-N1	1.245	1.240	1.240	1.241
O1-C2	1.346	1.351	1.351	1.351

Table A8 Selected geometry parameters for int_1, int_1', int_1'' and int_1'''

Dihedral angel	Compounds			
	Int_1	int_1'	int_1''	int_1'''
C1-C2-C3-N1	176.6	176.6	176.7	176.6
C3-N1-C4-C5	-153.4	-152.8	-153.2	-153.7
O1-C4-C5-C6	2.7	3.164	3.2	3.1
Bond length (Å°)				
N1-H2	1.007	1.007	1.007	1.007
N1-C4	1.452	1.450	1.451	1.452
C4-O1	1.423	1.424	1.424	1.423

Table A9 Selected geometry parameters for int_2, int_2', int_2'' and int_2'''

Dihedral angel	Compounds			
	Int_2	int_2'	int_2''	int_2'''
C1-C2-C3-N1	176.4	176.4	176.4	176.5
C3-N1-C4-C5	-175.0	-175.0	-174.9	-175.0
N1-C4-C5-C6	4.5	4.5	4.5	4.1
Bond length (Å°)				
N1-C4	1.282	1.282	1.282	1.283
N1-C3	1.404	1.405	1.405	1.404
C4-C5	1.468	1.467	1.467	1.466

Table A10 Selected geometry parameters for int_3, int_3', int_3'' and int_3'''

Dihedral angel	Compounds			
	Int_3	int_3'	int_3''	int_3'''
C1-N1-C2-C3	-28.0	-28.8	-28.2	-27.9
O1-C2-C4-C5	0.1	0.7	0.5	0.1
O1-C2-C3-H2	-54.4	-54.7	-54.8	-54.9
Bond length (Å°)				
N1-C2	1.451	1.452	1.452	1.451
C2-O1	1.441	1.440	1.441	1.442
O1-H1	0.973	0.973	0.973	0.973
H1-N1	2.444	2.449	2.450	2.445

Table A11 Selected geometry parameters for int_4, int_4', int_4'' and int_4'''

Dihedral angel	Compounds			
	Int_4	int_4'	int_4''	int_4'''
C1-C2-C3-C4	-65.2	-66.5	-66.9	-66.8
C3-C4-N1-C5	-50.6	-49.7	-49.5	-50.9
N1-C5-C6-C7	177.7	178.0	177.5	177.7
Bond length (Å°)				
C1-C5	3.480	3.479	3.489	3.500
C1-C2	1.353	1.353	1.353	1.353
C4-N1	1.408	1.408	1.408	1.407
N1-C5	1.278	1.278	1.278	1.279
C5-C6	1.470	1.470	1.469	1.468

สถาบันวิทยบริการ
จุฬาลงกรณ์มหาวิทยาลัย

Table A12 Selected geometry parameters for int_5, int_5', int_5'' and int_5'''

Dihedral angel	Compounds			
	Int_5	int_5'	int_5''	int_5'''
C1-C2-C3-C4	-8.6	-7.6	-7.7	-8.1
C3-C4-N1-C5	-3.2	-3.5	-3.4	-3.2
N1-C5-C6-C7	157.3	158.8	158.7	158.3
Bond length (A°)				
C1-C5	1.538	1.537	1.537	1.538
C1-C2	1.521	1.521	1.521	1.521
C4-N1	1.305	1.305	1.305	1.304
N1-C5	1.449	1.448	1.449	1.450
C5-C6	1.523	1.522	1.523	1.522

Table A13 Selected geometry parameters for int_6, int_6', int_6'' and int_6'''

Dihedral angel	Compounds			
	Int_6	int_6'	int_6''	int_6'''
C1-N1-C2-C3	-152.5	-152.4	-152.7	-152.7
H2-O1-C2-C3	-35.3	-39.3	-37.6	-35.7
C4-C5-C6-C7	-109.2	-103.0	-107.5	-107.7
Bond length (A°)				
H2-O1	0.967	0.967	0.967	0.967
C2-O1	1.452	1.452	1.452	1.452
N2-H1	1.013	1.013	1.013	1.013
N1-C2	1.462	1.462	1.462	1.463

Table A14 Selected geometry parameters for 1, 1', 1'' and 1'''

Bond length (A°)	Compounds			
	1	1'	1''	1'''
N1-H1	1.001	1.001	1.001	1.001
N1-H2	1.006	1.006	1.006	1.006
C1-N1	1.378	1.378	1.378	1.378

Table A15 Selected geometry parameters for 2, 2', 2'' and 2'''

Bond length (Å)	Compounds			
	2	2'	2''	2'''
C1-O1	1.219	1.218	1.219	1.220
C1-C2	1.481	1.480	1.479	1.478

Table A16 Selected geometry parameters for 3, 3', 3'' and 3'''

Bond length (Å)	Compounds			
	3	3'	3''	3'''
N1-H2	1.015	1.015	1.015	1.015

Table A17 Selected geometry parameters for 4, 4', 4'' and 4'''

Dihedral angle	Compounds			
	4	4'	4''	4'''
O1-C2-C4-C5	-150.5	-150.5	-150.5	-150.4
O1-C2-C3-C8	-3.5	-3.6	-3.5	-3.6
N2-C9-C3-C8	-179.2	-179.1	-179.1	-179.2
C4-C5-C6-C7	-105.1	-104.5	-105.6	-105.4
Bond length (Å)				
C2-O1	1.226	1.226	1.226	1.226

Table A18 Imaginary frequencies for transition states.

transition state	imaginary frequency, cm^{-1}
ts_1	-1723.01
ts_1'	-1715.46
ts_1''	-1717.06
ts_1'''	-1739.66
ts_2	-1754.97
ts_2'	-1743.17
ts_2''	-1728.57
ts_2'''	-1686.89
ts_3	-1571.44
ts_3'	-1570.00
ts_3''	-1568.91
ts_3'''	-1567.38
ts_4	-380.43
ts_4'	-387.12
ts_4''	-379.17
ts_4'''	-360.58
ts_5	-442.41
ts_5'	-441.53
ts_5''	-442.74
ts_5'''	-444.95
ts_6	-1034.22
ts_6'	-204.24
ts_6''	-186.43
ts_6'''	-201.12
ts_7	-1644.38
ts_7'	-1633.64
ts_7''	-1634.53
ts_7'''	-1636.96

สถาบันวิทยบริการ
จุฬาลงกรณ์มหาวิทยาลัย

VITA

NAME, NICKNAME: Mr. Parinya Hongtong

BIRTH DATE: November 6th, 1982.

BIRTH PLACE: Chachoengsao, Thailand

EDUCATION:

2001-2005: B.Sc. (Chemistry), Kasetsart University, Thailand.

2005-2008: M.S. (Petrochemistry and Polymer Science),
Chulalongkorn University, Thailand.

E-MAIL: teenoi_you@hotmail.com



สถาบันวิทยบริการ
จุฬาลงกรณ์มหาวิทยาลัย